Identification of Discontinuous Oil Bearing Sandstone Bodies by Direct Modeling: Risk Analysis for Well Planning

BY

Ahmad Atiq Mubarak Al-Dossary

MAY 2013

Identification of Discontinuous Oil Bearing Sandstone Bodies by Direct Modeling: Risk Analysis for Well Planning

BY

Ahmad Atig Mubarak Al-Dossary

A Thesis Presented to the

DEANSHIP OF GRADUATE STUDIES

KING FAHD UNIVERSITY OF PETROLEUM & MINERALS

DHAHRAN, SAUDI ARABIA

In Partial Fulfillment of the
Requirements for the Degree of

MASTER OF SCIENCE

In

GEOLOGY

May 2013

KING FAHD UNIVERSITY OF PETROLEUM & MINERALS
DHAHRAN 31261, SAUDI ARABIA

DEANSHIP OF GRADUATE STUDIES

This thesis, written by Ahmad Atig Mubarak Al-Dossary under the direction of his thesis advisor and approved by his thesis committee, has been presented to and accepted by the Dean of Graduate Studies, in partial fulfillment of the requirements for the degree of MASTER OF SCIENCE IN GEOLOGY.

Thesis Committee

Dr. Mohammad H. Makkawi
(Thesis Advisor)

Dr. Abdulaziz Al-Shaibani
Department Chairman

Dr. Khalid A. Al-Ramadan
(Member)

Dr. Salam A. Zummo
Dean of Graduate Studies

Dr. Mohammad A. Al-Khalifa
(Member)

11/6/13
Date

DEDICATION

To my father and mother, to my little family and to my country I dedicate this work.

ACKNOWLEDGEMENT

Acknowledgements are due to King Fahd University of Petroleum and Minerals for supporting this research and to Saudi Aramco for the permission to publish this thesis.

I would like to express my profound gratitude and appreciation to my thesis chairman, Dr. Mohammad Makkawi, for his guidance and for his critical review of the manuscript. Sincere thanks are also due to my thesis committee members, Dr. Khaled Ramadan and Dr. Mohammed Al-Khalifa, for their excellent advice and comments during this time and for their contribution to this work.

Appreciation and thanks are due to Chairman Dr. Abdulaziz Al-Shaibani and other faculty and colleagues of Earth Sciences Department for their support during my study.

I would like to thank the management of Saudi Aramco for providing the facilities and data used in this study. Of these I am especially grateful to Mr. Ahmad Q. Hameda, Chief Geologist of Northern Fields Characterization Division, and Dr. Ishak B. Ishak, Northern Offshore Area Group Leader. I am also grateful to Dr. Aus A. Al-Tawil, Manager of Reservoir Characterization Department, who dedicated himself to develop all the employee of his department equally. My thanks also go to my Specialist Development Program mentor Dr. Jose A. Vargas-Guzman for his continuous guidance and review of the thesis.

Finally, my sincere thanks are extended to my family and friends for their support and encouragement during the period of this study.

TABLE OF CONTENTS

Page

LIST OF TABLES

Page

LIST OF FIGURES

Page

THESIS ABSTRACT

NAME OF STUDENT: Ahmad Atig Mubarak Al-Dossary

TITLE OF STUDY: Identification of Discontinuous Oil Bearing Sandstone Bodies by Direct Modeling: Risk Analysis for Well Planning

MAJOR FIELD: Geology

DATE OF DEGREE: May 2013

The gigantic offshore clastic reservoirs in Saudi Arabia contain thick, prolific and continuous sandstone members; however, incremental development may include numerous laterally discontinuous prolific oil bearing sandstone bodies intercalated with non-reservoir rocks, in the so-called stringers. The optimization of hydrocarbon production requires advanced modeling workflows to identify and predict the spatial distribution of these clastic discontinuous rock bodies. This study proposes cross-validation of 3D models with new well bores to improve future predictions. The modeling approaches include sequence stratigraphy interpretations and identification of the depositional environment. Object-modeling, Indicator Kriging and sequential indicator simulation techniques were used to produce multiple realizations of 3D geocellular facies models that predict the geometry and location of sandstone bodies. New wells were planned and drilled based on the most probable predictions. Once a well is completed, actual data collected at the wellbore is compared to multiple geocellular realizations to evaluate an average error at each location. This error was later used to modify the facies model and workflows. The ultimate goal is to reduce uncertainty and optimize well planning.

Results are summarized to recommend corrections in the geological interpretation and modeling approaches. Based on results from this study, it was concluded that Indicator Kriging technique is the optimum way to predict rock bodies.

ملخص الرسالة

الاســــــــــم: أحمد عتيق مبارك آل فاران الدوسري

عنوان الرسالة: التعرف على أجسام الصخور الرملية المنفصلة والمحتوية على النفط عن طريق النمذجة المباشرة: تحليل المخاطر للمساعدة في تحديد مواقع جديدة لحفر الآبار

التخــــصــــص: الجيولوجيا

تاريخ التخرج: مايو ٢٠١٣

تحتوي مكامن النفط الضخمة والمتكونة من صخور رسوبية في المملكة العربية السعودية على صخور رملية سميكة ومتصلة مع بعضها ولكن مع زيادة الإنتاج من هذه المكامن فقد زادت وتيرة الحفر في صخور رملية محتوية على النفط تتميز بأنها غير سميكة ومنفصلة عن بعضها مما زاد من تحديات التخطيط للآبار المنتجة. إنتاج النفط الأمثل من هذه المكامن غير الاعتيادية يتطلب بناء نماذج جيولوجية قادرة على توقع مكان وعمق أجسام الصخور الرملية قليلة السمك بنسب مقبولة من الدقة. هذه الدراسة تقترح إختبار النماذج الجيولوجية ثلاثية الأبعاد ومقارنة دقة توقعاتها بنتائج عمليات الحفر الحديثة بهدف تحسين التوقعات المستقبلية.

النهج المتبع لبناء النماذج الجيولوجية في هذا البحث تضمن دراسة تتابع الطبقات والتعرف على بيئات الترسيب عبر فحص عينات الصخور المستخرجة من الآبار كما استخدمت ثلاث تقنيات جيوإحصائية لنمذجة هذه المكامن. بعد هذه الخطوة تم اختبار هذه النماذج باستخدام آبار حفرت حديثا وذلك لحساب مقدار الخطأ في توقعات النماذج والذي تم استخدامه لاحقا لإجراء تعديلات على النماذج. الهدف النهائي من هذه التعديلات هو تقليص مقدار الخطأ في توقعات النماذج وتحسين خطط الآبار الجديدة.

تتلخص نتائج هذاالبحث في في التوصية بتصحيح التوقعات الجيولوجية لنوعية الصخور وخطة بناء النموذج الجيولوجي بعد كل عملية حفر بئر جديد كما خلصت إلى نتيجة مفادها أن أحد التقنيات الجيوإحصائية المستخدمة في بناء النموذج الجيولوجي أظهرت نتائج أفضل من غيرها في توقع مكان وسماكة مكامن النفط.

CHAPTER 1

INTRODUCTION

1.1 Background

The largest clastic offshore reservoirs of Saudi Arabia are placed in members of the Cretaceous Wasia Formation (Hasson et al, 1977). The important reservoirs in these members are Safaniya and Khafji. Both have numerous laterally continuous and discontinuous layers of sand intercalated with shale and silts. The main units within the Safaniya and the Khafji members have continuous sandstone bodies that are prolific in terms of reservoir quality (Al-Sabti and Al-Bassam, 1993). Recent increase in oil demands created a need to develop production outside the main sand bodies and into the discontinuous bodies that are called stringers. The stringers are located at the bottom and the top of the main sand body, and they may be composed by complex and laterally discontinuous thin sand bodies. The risk of drilling in the stringers is high and would require geosteering to better predict the location of the sand bodies to ensure maximum

reservoir contact. This work is a contribution to the endeavor of mitigating risk while drilling by producing a probabilistic analysis for the occurrence of sand bodies. This work includes four major phases:

a) Data analysis and interpretation of clastic facies using logs and core data from wells.

b) Define the depositional environment.

c) Develop techniques to transform the lithological studies from logs into categorical facies that respond to an adequate depositional model.

d) Construction of geocellular models to characterize sand bodies and to help in their predictability using different modeling algorithms. For this purpose, the modeling techniques considered are: a) Indicator Kriging, b) Indicator Simulation and c) Boolean Object-based modeling.

The study focuses on applying the methodology and seeking practical solutions. The example presented is for the Safaniya member in a non-disclosed field. Data used in this study comes from Saudi Aramco, hence it is considered as confidential and must be sanitized. Therefore, information that can lead to the identification of this data set (i.e. depth, geographic location, …) have been removed. However, the thesis contains detailed information about the steps and techniques used. This research topic is of a general interest to both academia and industry.

1.2 Problem

One of the main challenges associated with developing hydrocarbon production from Safaniya and Khafji members is to predict the location and the geometry of sandstone bodies in the subsurface. The special position and the size of sandstone bodies is highly uncertain, particularly in the stringers (Hashem et al, 2008). In an ideal case, drilling a horizontal well in a clean and relatively thick sand stringer will result in a hundred percent reservoir contact. In practice, however, this result is seldom achieved. This is due to the difficulty of identifying facies from logs and poor predictability of sand body's geometries between wells. This leads to difficulty in keeping the well path within a sand body while drilling a horizontal well in these stringers. The complexity of deltaic environments, similar to which Safaniya and Khafji members were deposited, is observed in Figure 1.

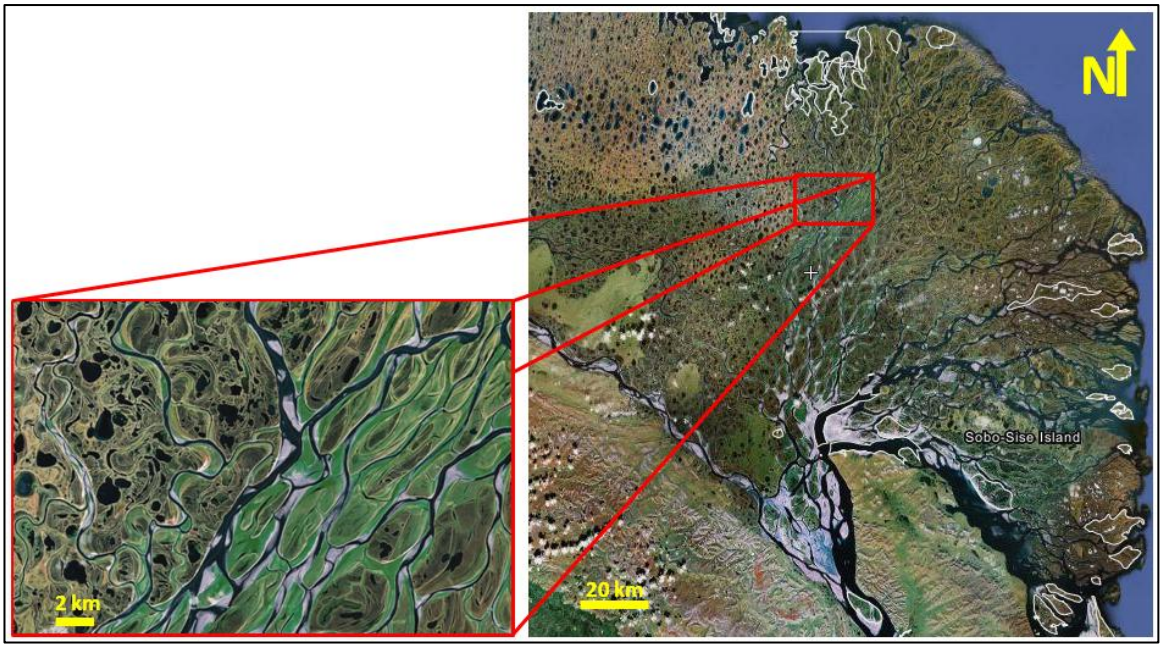

Figure 1 Lena Delta in Russia is an example of a complex deltaic system. It has different sizes, lengths and orientations of the distributary channels and mouth bars. The small box shows the hetrogenity that may be encountered while drilling a horizontal well (modified after Olariu and Bhattacharya, 2006).

1.3 Objective and Proposed Solution

This study attempts to develop a methodology for identifying and characterizing sandstones bodies from well data, core data and analogs by using geostatistical modeling, which eventually leads to the construction of geocellular models. The work is a contribution to the endeavor of mitigating risk while drilling by producing a probabilistic analysis of the occurrence of sand bodies. It is a well-known fact of nature that sandstone bodies follow physical laws of deposition. The study of sedimentation, accommodation, tectonism, and the use of outcrops and modern analogs has helped researchers to identify the possible geometries of sandstone bodies in the subsurface (Pettijohn et al, 1987). The prediction of sandstone bodies at non-sampled locations should follow scientific logic. However, due to geological heterogeneity, it is not possible to predict the geometry of a specific sandstone body from well data only. The use of seismic data is constrained to availability and resolution. This study, however, focuses on the use of well logs, core data and analogs to define objects that can be derived from the existing data.

Heterogeneity of complex sandstone bodies is directly related to the environments of deposition, hence quantitative assessments and 3D modeling is required to have a realistic prediction for size and geometry of sandstone bodies (Al Maskeen, 2007). In this study, three workflow algorithms are utilized: a) Indicator Kriging b) Indicator Simulation and c) Boolean Object Modeling. These techniques do not provide exact or "magic" predictions of the sandstone bodies; instead, the first one generates a smooth model and the last two provide several possible realizations, conditioned to well data and analogs. Those multiple realizations allow for computation of the probability of success of

horizontal wells to remain within prolific zones. One has to note that geosteering horizontal wells using logging while drilling (LWD) and modeling while drilling is currently done in localized sector models without reinterpreting the whole field geology (Georgsen et al, 2008). The workflow in this thesis was to produce a quantitative method to capitalize on the errors found while drilling by modifying the existing geological conceptual and numerical models for planning new well paths in an iterative fashion.

1.4 Dataset Description

A non-disclosed field from the northern offshore area (Figure 2) was selected to conduct this study. A total number of 13 wells representing the whole field (Figure 3) were released by Saudi Aramco to be used in the context of this thesis. In addition to the cored wells, 188 logged wells were used to populate the facies in non-cored wells and then to build the 3D model. For quality control, 31 logged wells and 3 cored wells were used to validate the model predictability but they were not used in the modeling phase. The cores cut in the thirteen wells have different lengths and cover different facies. These cores are used to define the depositional facies of Safaniya member. The available logs include: Gamma Ray (GR), Density (RHOB), Neutron (NPHI), Photoelectric Factor (PEF), Sonic (DT), Effective Porosity (PHIE) and Shale Volume (VSH).

The well logs and directional surveys were loaded into a Petrel 2012.4 project, which is the modeling package used in this study. Petrel package was installed on a 32-bit Dell PC machine with 2 Gigabyte of Random Access Memory (RAM), 3.2 GHz Intel processer and 256 Megabyte graphics card.

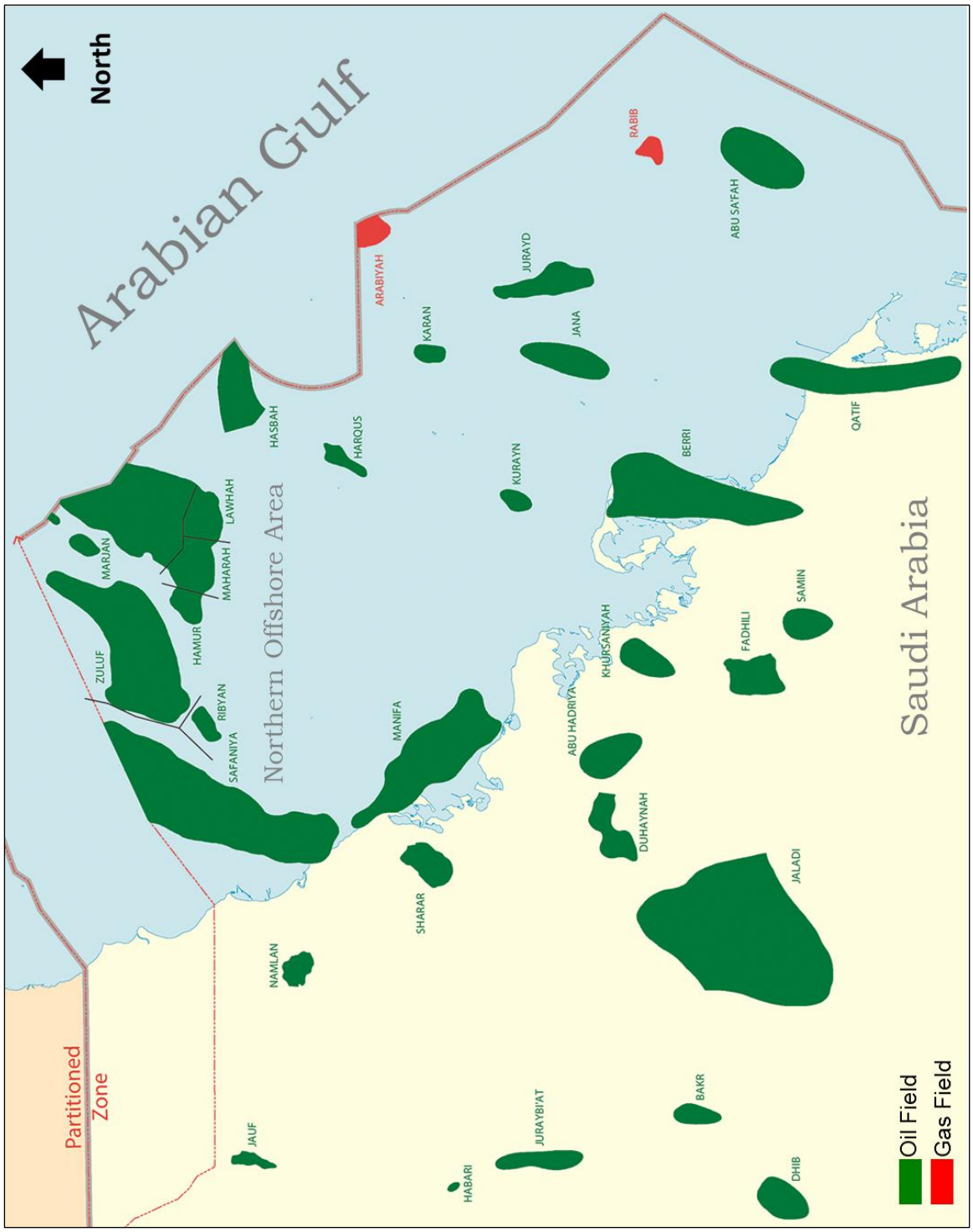

Figure 2 Location map of the northern offshore area fields (modified from Al-Ghamdi et al, 2001).

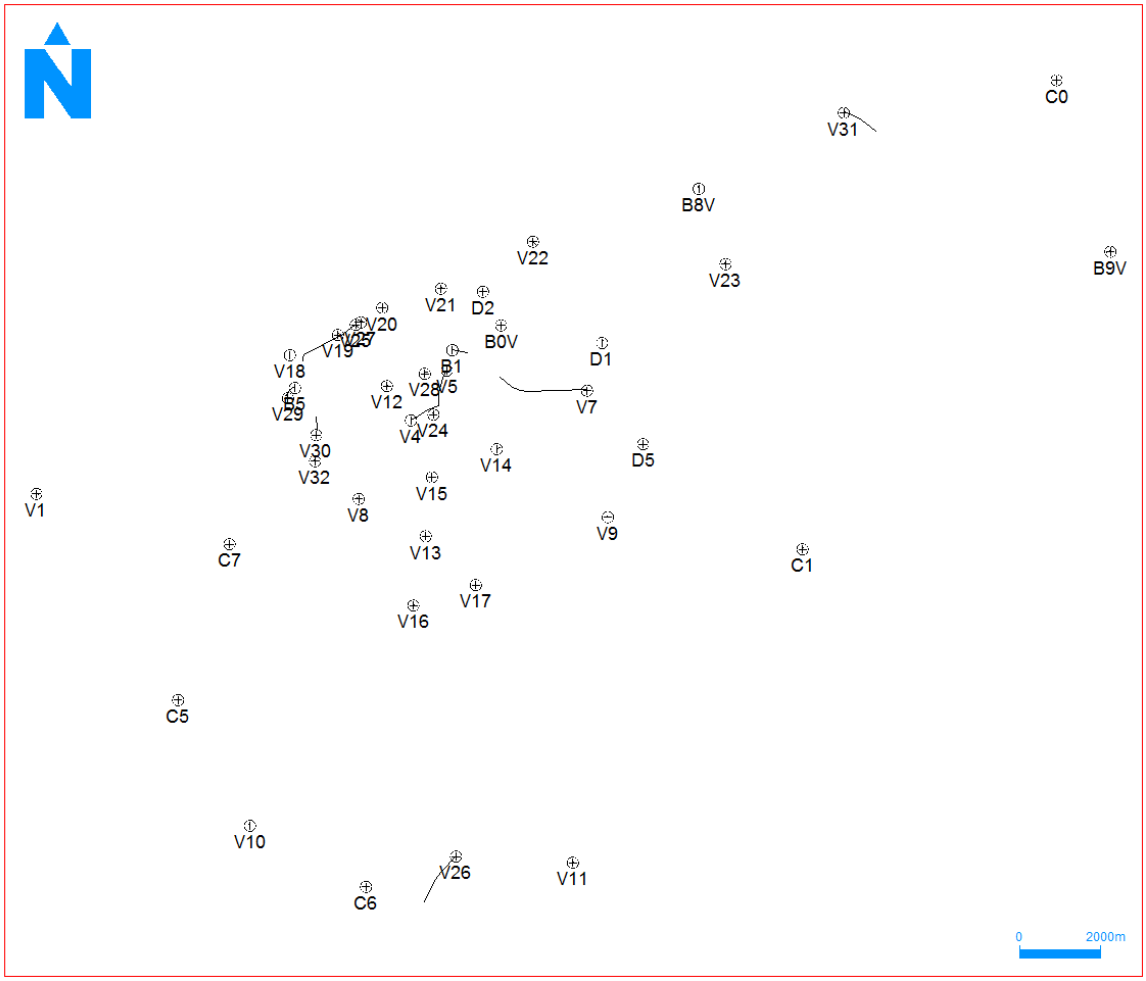

Figure 3 A map of the relative positions of the 13 cored wells (B1, B5, C0, C1, C5, C6, C7, D1, D2, D5, B0V, B8V, B9V) used in this research and the 31 wells used to validate the model predictably (denoted by the letter V).

CHAPTER 2

LITERATURE REVIEW

2.1 Geological Review

2.1.1 Regional Geology

Safaniya member was deposited during the tectono-stratigraphic mega-sequence (TMS) AP8 that dominated the Arabian plate and lasted some 57 million years (between149 and 92 Million years ago; Figure 4). The base of this TMS is marked by widespread unconformity hiatus surface that overlies the evaporite deposits of Hith Formation which resulted from gentle uplift structuring in the north and a relative fall in sea level. The top of this TMS is marked by the Pre-Aruma unconformity that resulted from a localized uplift and possibly a global eustatic fall in sea level. During this TMS the Arabian Plate was essentially stationary in an equatorial position and the plate was dominated by generally rising global sea levels. As a result, the accommodation space was increasing and sometimes the clastic sediments prograded as a result of the hinterland uplift in the west. The clastic Safaniya and Khafji members of Wasia Formation and

similarly Biyadh Formation were very strongly progradational then in a later period they started to retrograde as a result of the onset of hinterland erosion that diminished sediments. (Sharland et al, 2001)

Fifteen maximum flooding surfaces (MFS) are recognized in the TMS numbered AP8 (Sharland et al, 2001). The focus will be the time period between MFS number K90 and MFS number K110, within which the Khafji and the Safaniya members were deposited (Figure 4). During this time period Khafji, Safaniya, Mauddud members and their regional equivalents were deposited. The start of this period was after the late-Aptian regional unconformity and sedimentary hiatus which separated rocks of the Albian age Wasia Formation from Aptian age Shu'aiba Formation (Ziegler, 2001). This unconformity coincides with a worldwide lowstand in sea level (Haq et al, 1988) during which the Khafji member was deposited. The sedimentary hiatus was then followed by a period of rising sea level that resulted in the deposition of Dair limestone during a maximum flooding surface event (K100). Safaniya member was then deposited during a drop in sea level and finally followed by a sea level rise during the maximum flooding surface K110 that resulted in the deposition of Mauddud member by end of Albian (Ziegler, 2001 and Sharland et al, 2001) (Figure 5).

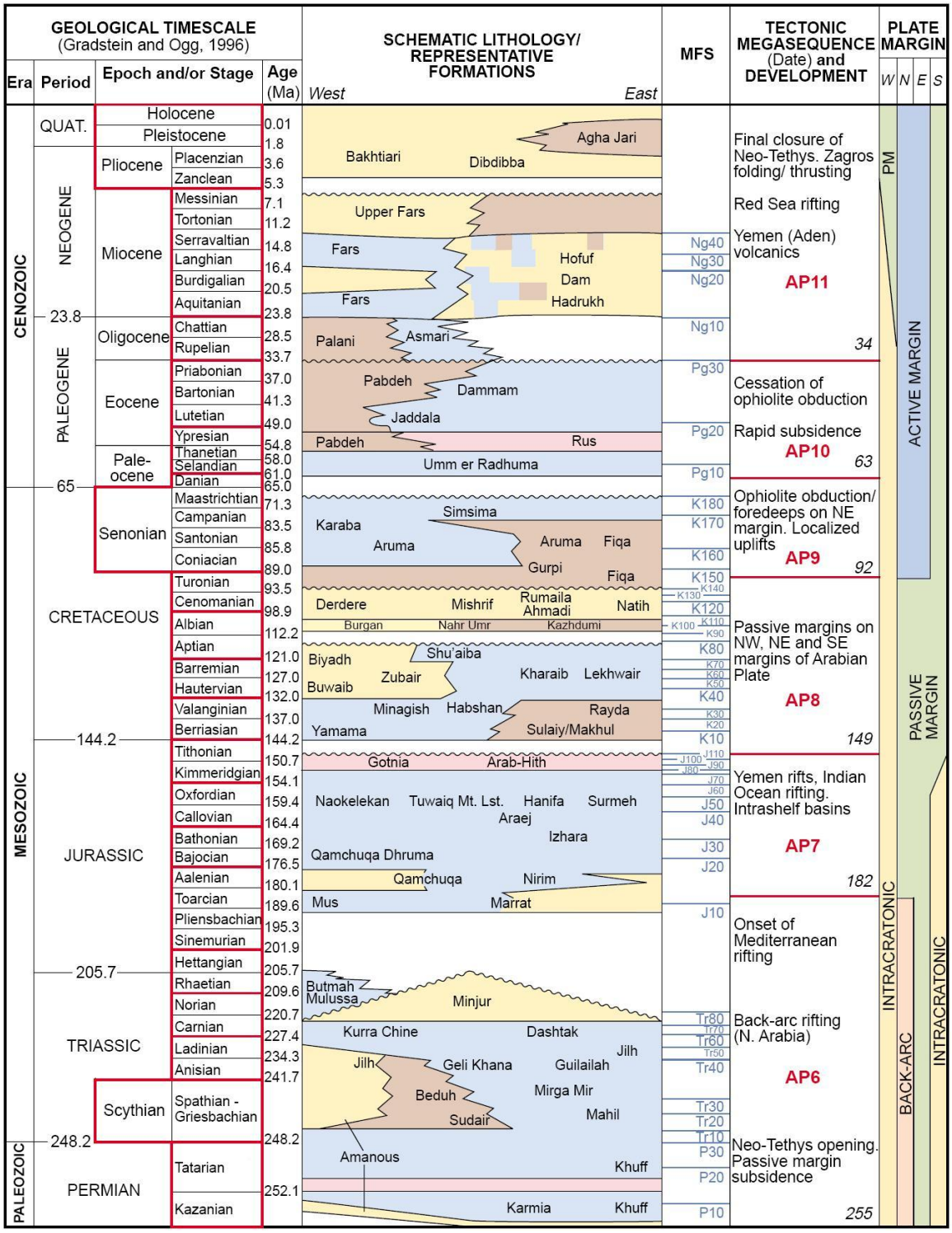

Figure 4 Stratigraphic column showing the tectonostratigraphic mega-sequence AP8 and its relative age to the other mega-sequences, modified from Ziegler (2001).

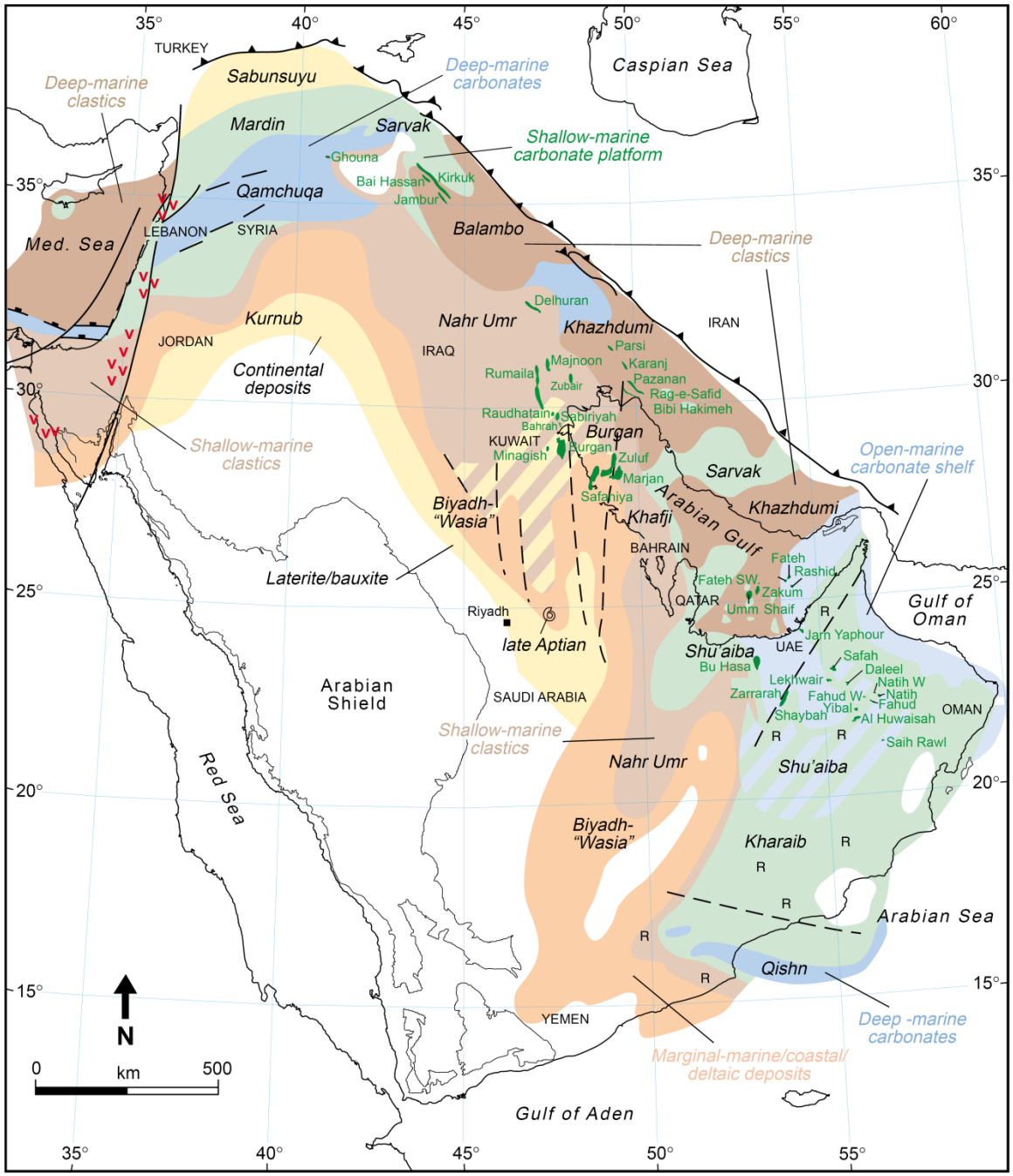

Figure 5 A map showing the distribution of the major regional formations and their depositional environments during the Late Early Cretaceous 121-98.9 Ma. During this time period the northern offshore area was dominated by marginal marine, costal and deltaic deposits (Ziegler, 2001).

2.1.2 Geology of the Khafji and the Safaniya members

In the northern offshore area, Khafji and Safaniya members are mainly clastic and were interpreted as fluvial dominated delta deposits (Chevron, 1990). The Khafji member is divided into three main units, the lower stringers, the main sand and the upper stringers (Figure 6). The lower stringers were deposited during a drop in the sea level where prograding deltaic clastics were deposited on top of shallow marine sediments. The main Khafji sand is a low stand deposit that deposited in a high energy braided river system. It is characterized by massively bedded sandstone that contains small amount of thin shales formed after flooding events. The upper stringers were deposited during a sea level rise and consist mainly of meandering stream deposits. Sand in this environment is typically deposited in point bars formed at river bends (Mashhadi, 1998).

The same sequence stratigraphic cycle is repeated in the Safaniya member. The lower stringers of Safaniya member was deposited in shallow marine environment to marginal marine bays with minor distal mouth bars and splays. It is mainly composed of shales with minor sandstone. The main sand bodies were deposited in distributary channels and mouth bars. Those bodies are composed mainly of massive sandstone. The upper Safaniya member was deposited in inter-distributary bay and splays and composed mainly of shale and minor sandstone (Al-Sabti and Al-Bassam, 1993; Figure 6).

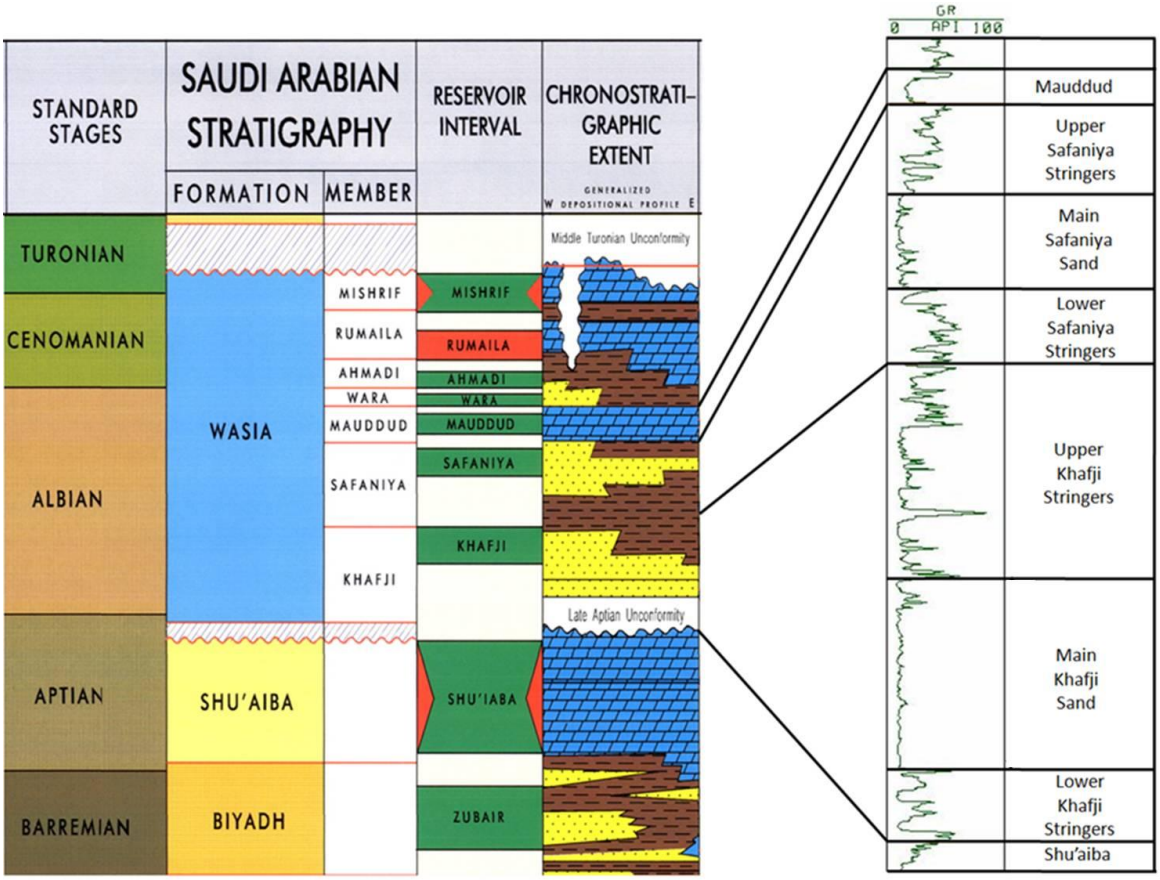

Figure 6 Stratigraphic column and typical gamma-ray log of the Safaniya and Khafji members (Wasia Formation) in northern offshore area. The lower stringers and the main sand section in both members are generally coarsening upward where the upper stringers in both members is a fining upward section .

Generally, the sand quality and quantity in the Safaniya and the Khafji members deteriorate as traversed from southwest toward the northeast of the northern offshore area (Figure 2). The studied core lithofacies show that southwestern part is dominated by sand deposited in channels and mouth bars, whereas the northeastern part dominated by splays and bay deposits (Chevron, 1990; Figure 7)

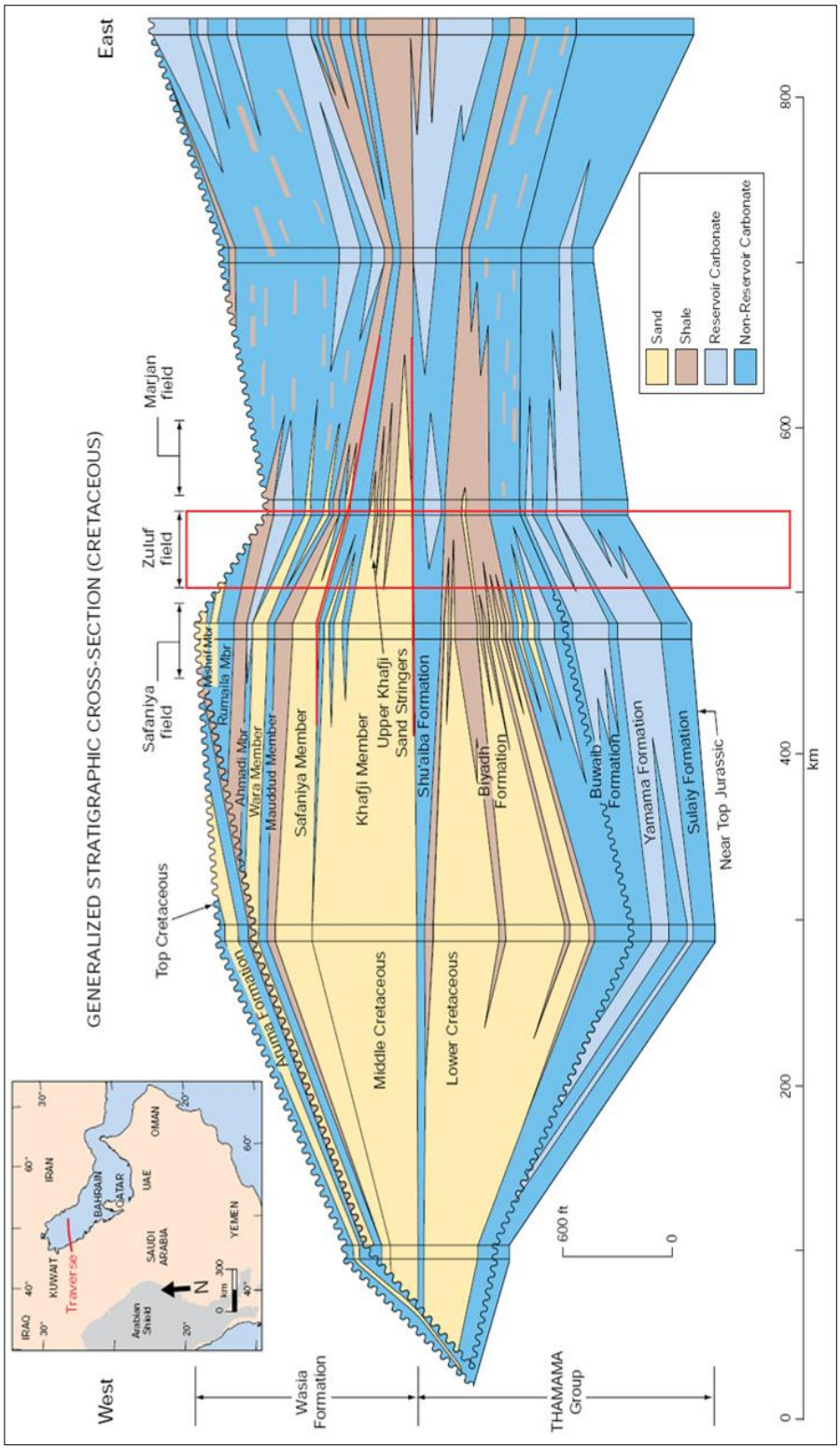

Figure 7 Generalized stratigraphic cross-section of the Cretaceous in the study area (after Macrides and Neves, 2008).

2.2 Geocellular Modeling

In this research; three modeling methods are used to model the facies: Indicator Kriging (IK), Sequential Indicator Simulation (SIS) and Object-Based modeling. IK and SIS are the standard methods currently used to build geological facies models for Safaniya and Khafji members in Saudi Aramco. Object-based modeling has not become standard tool yet, because it requires recognition of facies geometries from the well logs. Recognizing a facies or a depositional environment from well logs is not impossible but it is rather uncertain because many facies and depositional environments share the same log response (Rider, 1996). For that reason, further studies are needed to define facies from core data and then define facies in uncored wells. In this research, an approach was tested to predict the facies from well logs and it will be discussed in Chapter Four.

2.2.1 Indicator Kriging (IK)

Indicator kriging is a spatial estimation method performed on a binary-transformed (i.e. indicator) sample set. A selected rock category is coded as 1 if it is present at a given location otherwise it is coded zero. The indicator kriging approach was first proposed by Journel (1983). Indicator kriging has also been used for highly variant (non-Gaussian) continuous properties discretized or converted into categorical categories. If a variable lies above or below a defined cutoff value it is treated as categorical variable or indicator. The method is also called non-parametric estimation. Other useful applications are the modeling of categorical variables, e.g. if a sample belongs to a certain facies type.

The approach in this research is the use of ordinary-indicator kriging as it significantly reduces the smoothing effect. Note that simple indicator kriging requires a constant mean which is a stronger stationarity constraint that can over smooth a facies model (Marinoni, 2003). Ordinary indicator kriging also implies an overall constant mean which is not used in the computations. Therefore it allows for local variations in the proportions of rocks. It is worth to mention that indicators have interesting properties. One of which is that the mean or expected value of indicators is equal to the proportion of the category or facies. Another relevant property is that the variance of an indicator random variable can be written in terms of proportions. This aspect is critical, because the right variance of a facies category implies the mean is also correct and in consequence the proportion of rocks and reserves are also correctly estimated. The lack of this knowledge leads to unstable models with too much variability and wrong proportions. The other extreme is to have smoothing effects that lead to wrong proportions of rocks as well. Insight and details on advanced use of indicators can be found in the literature (Deutsch and Journel, 1998).

Indicator kriging provides the best linear unbiased estimator for the expected value or local spatial average proportion (or probability) of certain facies occurring at a given location. The estimated values are converted into actual rock categories by comparing the estimated probabilities to the average (expected) proportions. However, the final estimates cannot represent the overall heterogeneity as observed in actual outcrops. In addition, smoothing effects of kriging are in general unavoidable unless one simulates the remaining heterogeneity, which will be explained in the next section.

2.2.2 Sequential Indicator Simulation (SIS)

Sequential Indicator Simulation is the integration of an IK estimate and a simulated residual. The approach requires careful handling because it can generate random artifacts, and unstable results. Hence, the relation of the sill of the indicator semi-variogram (i.e. indicator variance) and the proportions of rocks needs to be observed to obtain valid, stable and reasonably continuous simulated rock regions. One must avoid getting fractal looking realizations which indicate mathematical instability in the algorithm. Some people however have used this disadvantage to forecast highly heterogeneous reservoirs affected by diagenesis (Deutsch, 2002). The results have high variability but accurate anisotropy and semi-variogram measures of spatial correlation. Sequential Indicator Simulation involves randomly visiting each grid node in the model domain. At each node in the grid, a facies code is assigned as per the following steps:

1. Find data and previously simulated grid nodes close to the predicted location to be simulated. This is called a neighborhood.

2. Construct the conditional distribution by estimating the local probability parameters by indicator kriging.

3. Use a random number generator to sample from the conditional distribution

4. Evaluate the probability of each facies being present at the current location in comparison to the expected parameters

5. Draw a simulated facies from the most probable outcome of the set of probabilities and assign it to the node

Repeating this entire procedure will result in generating one realization. I addition, using different random number seeds is utilized in generating multiple realizations for the modeled domain (Deutsch, 2002).

2.2.3 Object-Based Modeling (OBM)

Object based model is also called "Boolean" models in the literature. These models are visually attractive because they mimic idealized geological objects geometries interpreted in outcrops and modern analogues. These techniques are used to model geological objects with realistic geometries which cannot be predicted using linear indicator approaches (i.e., IK and SIS) (Deutsch, 2002). This modeling approach depends on object geometry and statistical information about the size used to model each type of sand bodies. Their thicknesses may be generated statistically from the thickness histogram of bodies encountered at wells. Their width can be derived from their size using width-thickness relationship charts (Gibling, 2006). Another important quantitative constraint is the total proportion of each type of individual body present in the total reservoir volume. This is often derived from the objects proportions calculated from the wells (Dubrule, 1998).

OBM is usually used in modeling fluvial channels as they have certain geometries and dimensions that could be simulated from modern analogs and be reproduced mathematically. The workflows of modeling and positioning fluvial facies objects are shown in figures 8 and 9 (Deutsch, 2002).

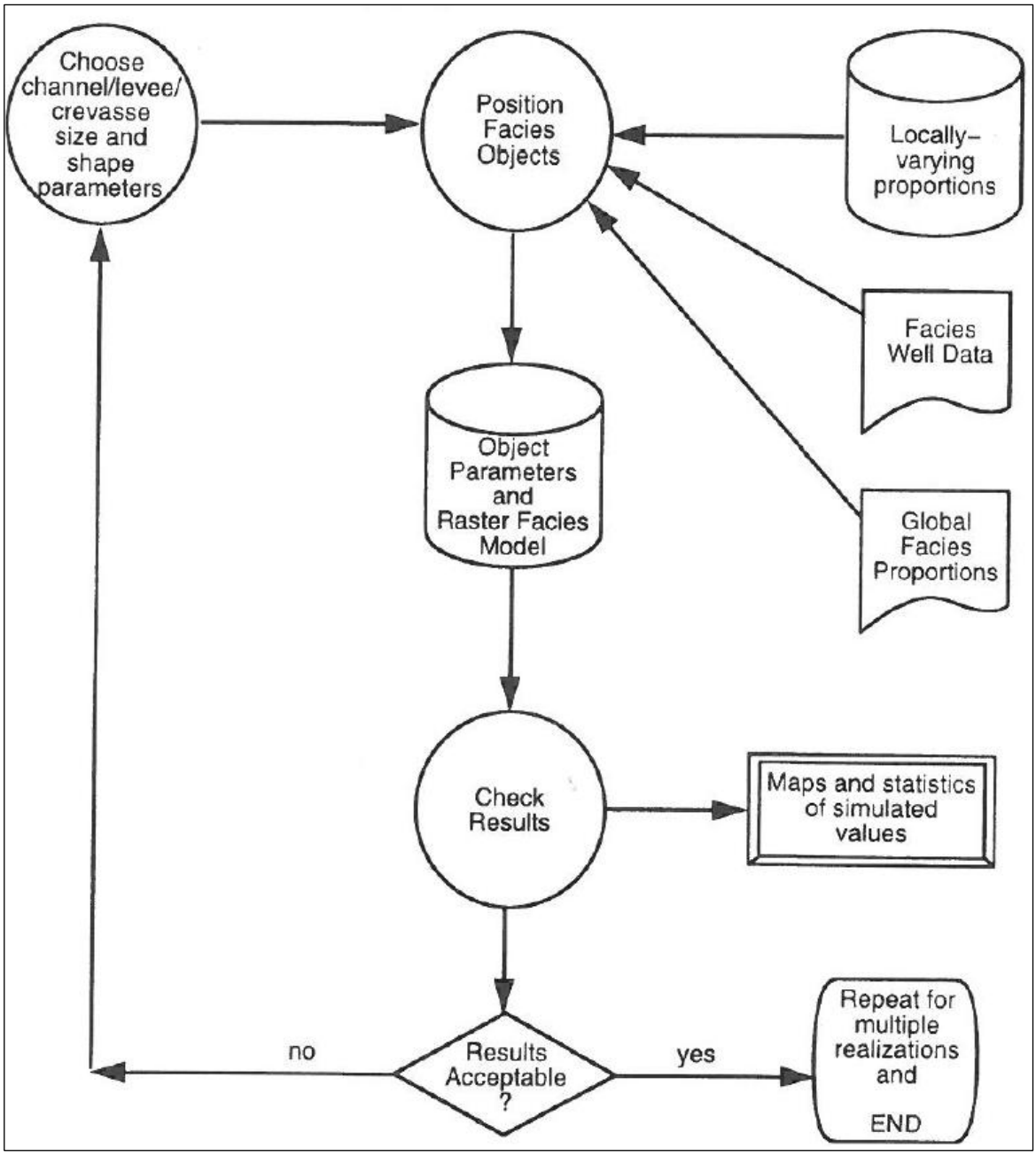

Figure 8 Workflow of modeling fluvial facies objects (Deutsch, 2002).

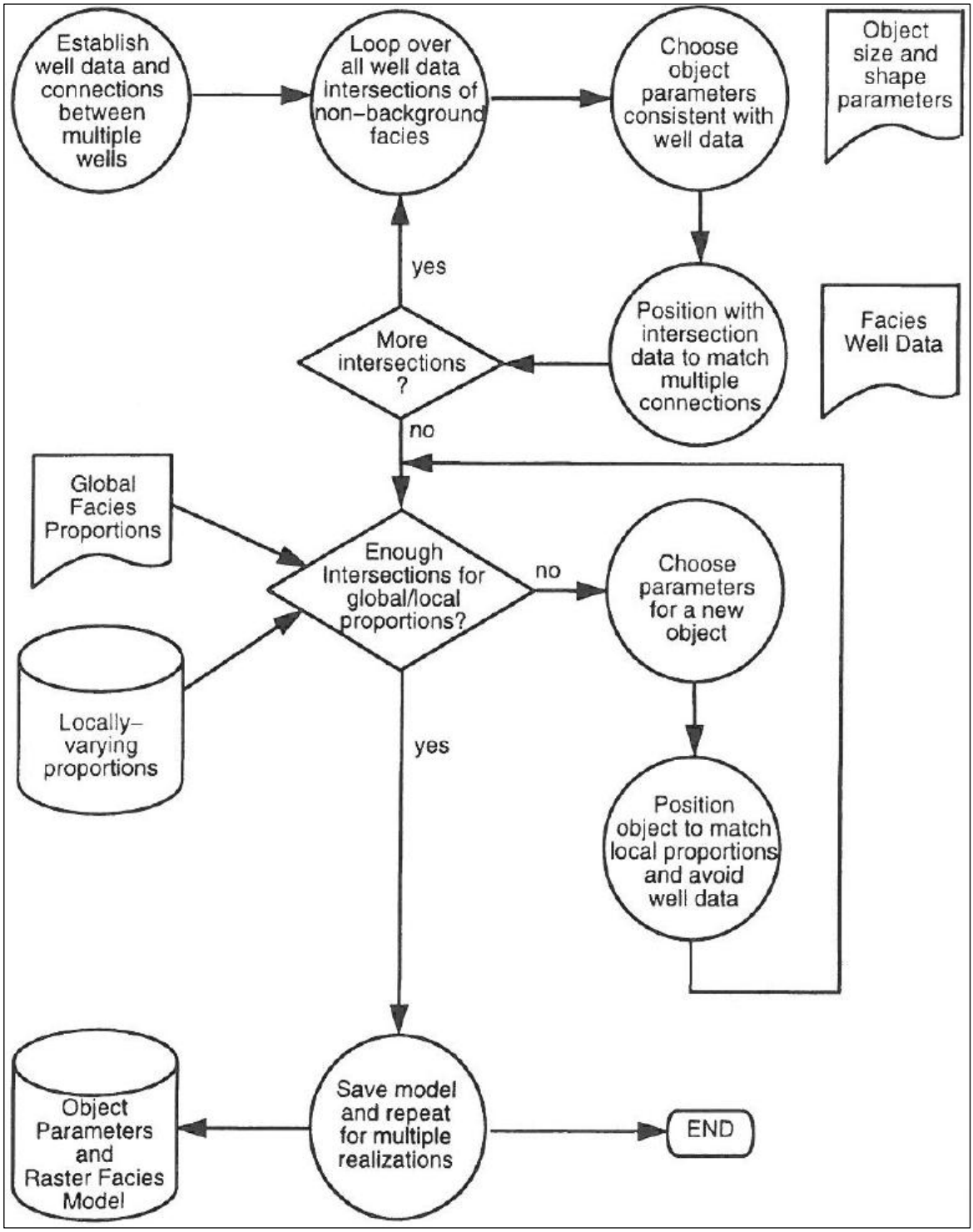

Figure 9 Workflow of positioning facies objects into the model (Deutsch, 2002).

2.3 Alternative Technologies and Solutions

Several methods were tested and applied to reduce the uncertainty of sand body's geometry in the subsurface. One technique is the amplitude variation with angle (AVA) seismic inversion. This technique can image sand bodies in the subsurface and define their geometries (Contreras et al, 2005). However, there are two main limitations for this approach: first, a 3-D seismic volume must exist, and secondly the lack of high resolution to image thin sandstone bodies. This may lead to missing thin-sand bodies (less than 30 feet in thickness), which is generally more than the thickness of the stringers.

Strebelle (2002) has developed an algorithm based on multiple-point statistics (MPS) to simulate categorical attributes, e.g. geological facies, and has been tested to simulate a 2-D fluvial reservoir. This method used two training images which have been drawn and digitized. The author concluded that in contrast to object-based modeling techniques, the developed algorithm allows simulation of any type of geological heterogeneity, of any shape, at any scale. However, this approach will not be considered in this research due the lack of training images compatible with well data as required by the algorithm. The selection of analog image may lead to whole quantitative study, and the tool for such a task is not available from the MPS researchers yet.

Vargas-Guzman and Qassab (2006) introduced a new approach for modeling complex clastic reservoirs by generating updated probabilities using residuals from sequential indicator kriging then integrating them in object modeling. The technique was applied to a Devonian reservoir in Saudi Arabia defined with nine facies categories. The facies object shapes were provided by a geologist and were modeled accordingly. The

study concluded that this new approach of grouping indicator random fields in geo-objects can be applied on other reservoirs and fields. A significant advantage of the approach is that objects are no longer randomly placed but they follow spatially correlated constraints.

Busch and Link (1985) and Rider (1996) explained that Gamma ray and some other electrical logs can be carefully used to indicate depositional environment facies (see Figure 8) which can be then used to predict the facies distribution and extent. This approach assumes that knowledge about the depositional environment could be derived from cores or outcrop analogs. The reason for that is the shape-overlap between several logs in different depositional environments.

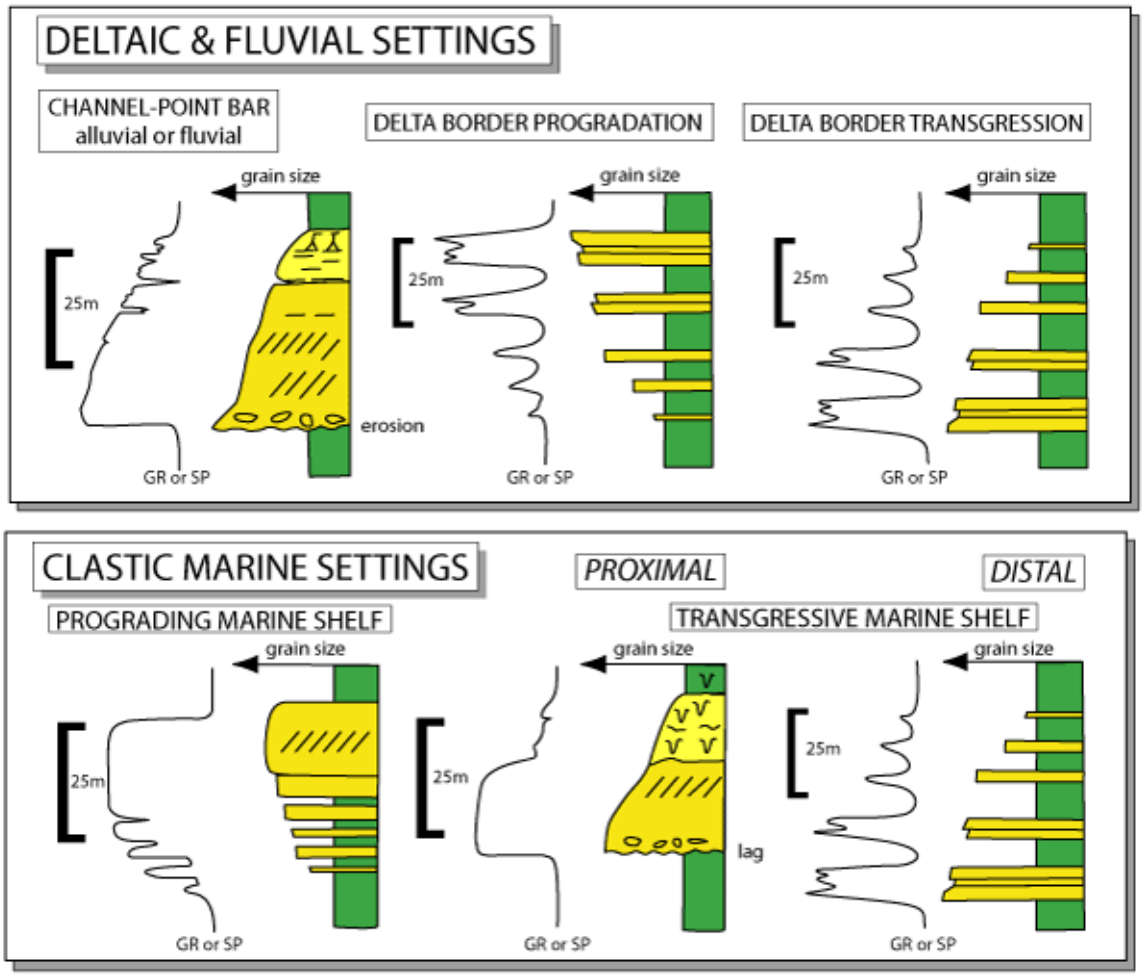

Figure 10 Facies indications from gamma ray (or SP) log shapes. These are idealized examples for log shapes and sedimentological facies (modified after Rider, 1996).

Reservoir data conventionally are acquired with well logs and cores. These data, however, generally are not enough to generate an accurate model of the reservoir. Al-Khalifah and Makkawi (2002) assessed the significance of incorporating different types of data (such as seismic acoustic impedance and depositional facies) with 3-D geostatistical porosity models. They concluded that in high-density wells areas, the well control can be sufficient to give good prediction. Whereas in sparse areas; well spacing and other data are needed to improve the prediction.

According to Tye (2004), the greatest uncertainty in subsurface interpretations is the inter-well distribution, continuity, and connectivity of sandstone bodies. Combining core and wire-line log data (vertical) with dimensional measurements from geomorphic analogs (Spatial) creates a fully three-dimensional data set. Using statistical distributions of length, width, and orientation of modern sedimentary environments as input for numerical models decreases geologic uncertainty and provides a method for probabilistic testing.

Saggaf and Nebrija (2000, 2003) used the fuzzy logic approach to estimate the depositional facies and lithology from wire-line logs in non-cored wells. This approach is very useful, because it provides a confidence measure that can be used to assess the quality of the analysis made. The technique was tested on a cored well and the results then were compared with facies derived from core analysis. Results from the two wells showed considerable agreement, which indicate that this method can be used effectively to predict the facies of uncored wells from their logs. This approach was used in this research to estimates the depositional facies in non-cored wells as will be discussed in Chapter Three.

CHAPTER 3

CHARACTERIZATION STUDY

3.1 Core Description

In this study, thirteen cored wells have been used for lithology and depositional environments identification (Figure 3). Eleven of them were studied by Chevron Services Company between the years 1983 and 1990 and the other two wells were studied and described by Saudi Aramco sedimentologist in 2009 (Appendix A). These available core descriptions are used to generally classify the depositional environments observed in Mauddud and Safaniya member and their distribution through the field. These classifications are very important to help in predicting the shape and geometry of the geobodies that are modeled in the next part of this research. For example, assigning channel facies to a specific interval of the core will give an idea about the thickness and width of a channel. If that specific data is integrated with nearby wells data, it can give an idea about the orientation of channels.

Results from core description revealed six general types of depositional systems that contributed in the deposition of the Safaniya member, which are: channel, splay, mouth bar, bay, swamp and marine (Figure 9). It was noticed that in the southern part of the field there was a dominance of fluvial channels facies that gradually changes into marine as we traverse toward the northeast. This indicates that the most proximal source of the channels in the field was located in the southwestern part of it.

Code	Name	Color
1	Channel	
2	Splay	
3	Bay	
4	Mouth Bar	
5	Swamp	
6	Marine	

Figure 11 The main six depositional facies identified from core description.

The lithology of Safaniya member is mainly composed of clastics with some carbonate rocks particularly in the northeastern part of the field. The lithology types presented in Safaniya member are classified as follows: clean sandstone, sandstone, shaly sandstone, shale, coal and limestone. Mauddud member is mainly composed of limestone, which gets thicker toward the northeast, and shale while the Safaniya member sands gets thinner and having more shale towards the northeast.

3.2 Facies Prediction

In order to build a 3D geocellular model; a good number of wells should have appropriate facies and lithologies interpretation otherwise uncertainty will be high. This "good" number means representing all or most of the depositional facies and their variation in both vertical and lateral dimensions. After identifying the main depositional facies and lithologies of Safaniya and Mauddud members in the thirteen cored wells; the next step is to predict the facies in the 188 non-cored wells. This task was performed using artificial neural network technique which is embedded in Petrel version 2009.1.

Neural network is a tool used to determine lithofacies and other rock properties from well logs. There are several learning algorithms in this tool, but the most popular is "back propagation" algorithm. This algorithm got its name from its method of propagating errors backwards through the network. The training algorithm consists of two main steps: feeding forward and back propagation (Ali, 1994).

If sufficient data are used for training the network then neural networks will learn from their past experiences. Back propagation involves sending the input pattern forward through the network, and then computing the output error resulting from the difference between the actual output and desired output. New set of weights are repeatedly calculated to minimize the error until the desired output is obtained (Rogers et al, 1992). Associated mathematical equations are in (Appendix B).

This tool was used in this study to identify the relationship between facies and the other measured logs that include Density (RHOB), Neutron (NPHI), calculated Volume of Shale (VSH) and effective porosity (PHIE) logs.

The workflow for predicting the six facies of Safaniya and Mauddud members in the non-cored wells using neural network was:

1. Choosing ten cored wells with facies interpretation and using them to supervise and train the estimation model
2. Selecting the logs associated with all the ten cored wells: RHOB, NPHI, VSH and PHIE
3. Setting the maximum number of iteration at fifty and setting the error limit at ten percent
4. Conditioning the percentage of the supervised data that were used in cross validation to 50%. The remaining points were used for training
5. Checking the correlation table for each facies and deciding about appropriateness to predict facies or not

The first trail run reviled that the swamp facies have very low correlation values indicating that it may not be estimated with high confidence. The reason for that is the swamp facies are localized and have very small thickness. In other words, training the neural network needs more data that swamp facies category does not really have. Mouth bar, splay and channel facies also had relatively low correlation values except in the case of PHIE and VSH logs. These two logs are directly indicating very common properties of the channels and mouthbars facies which are: noticeably low VSH and high PHIE. The

low correlation with other logs could be due to common log characters between the three facies that are mainly composed of sandstone with small or no shale contents. Bay facies could be predicted with higher confidence by all logs except the RHOB log, and marine facies are relatively best predicted using RHOB and NPHI logs (Table 1). It was clear that the estimation model could not be run properly because some of the facies could not be predicted correctly and due to mixing between facies signature.

	Channel	Splay	Bay	Mouth Bar	Swamp	Marine
NPHI	0.3636	0.1388	0.5018	0.1216	0.0484	0.2137
PHIE	0.4822	0.2725	0.6723	0.1849	0.0037	0.0676
RHOB	0.1408	0.1053	0.0001	0.0260	0.0315	0.2149
VSH	0.4644	0.2840	0.6883	0.1680	0.0140	0.0681
Total	0.5447	0.3072	0.7101	0.1929	0.0589	0.3495

Table 1 Correlation coefficients of the six depositional facies with well logs.

To solve this problem it was necessary to reduce the number of deposional facies by grouping them into general facies categories. To do that; channels, splays and mouthbar facies were put under one category that is fluvial. The swamp facies was eliminated because it was not significant – based on well data – in terms of its proportion and volume in the field, which is less than 1%. Bay and marine facies were kept as they are. The coorelation coefficient analysis showed higher values indicating better predictability and estimation of depositional facies in non-cored wells (Table 2). This is due to the fact that minimizing the number of facies that are having similar log characteristics leads to better training neural network estimation algorithm. In chapter 4 of this study, more elaboration on the derivation of fluvial channels, bay and marine facies proportions in each zone of the model.

	Fluvial Channel	Bay	Marine
NPHI	0.1873	0.5748	0.5877
PHIE	0.6780	0.5649	0.1407
RHOB	0.1510	0.1625	0.4627
VSH	0.5429	0.7138	0.2787
Total	0.6849	0.7337	0.7327

Table 2 Correlation coefficients of the three generalized depositional facies with well logs.

The Estimation model was run to predict the facies in non-cored wells and the results were found close to the reality in most of them but in some cases it gave few erratic predictions. For example, some thin sandstone layers were predicted within the limestone and vise-versa. This error might be due to similarities of the log characters between clean sandstone and porous limestone which both have generally lower density and higher porosity. The next step then was to quality check the facies predictions in all 188 non-cored wells and manually edit and correct the error in every single well, if applicaple besed on nearby cored wells and knowledge of visual log interpretation gained from field experience (Figure 10).

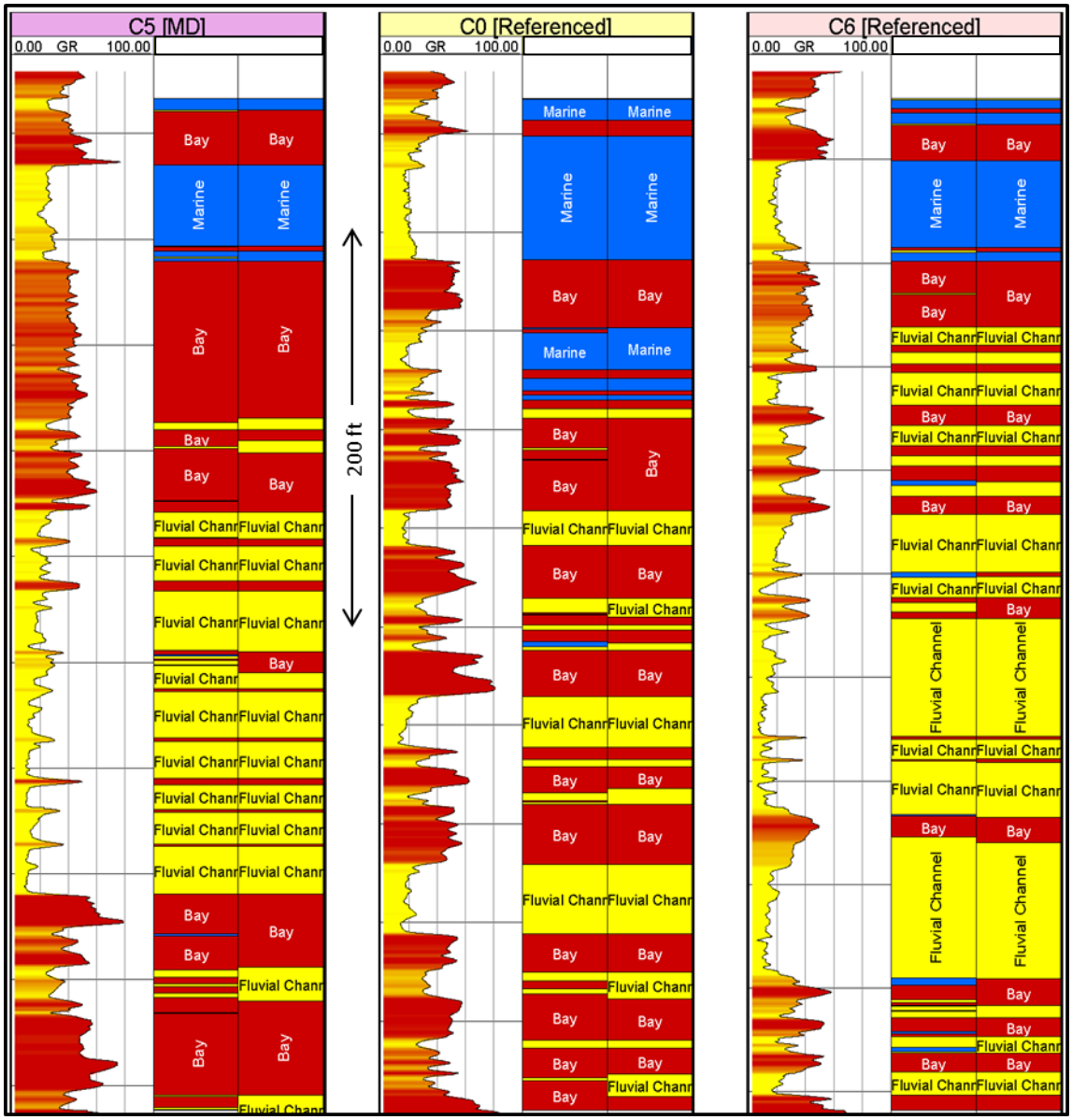

Figure 12 Examples of neural network depositional facies prediction in three wells. The first track contains the Gamma ray log with a scale from 0-100 API. Second track contains the initial prediction that needed to be corrected and manually edited as some of the facies like the marine (blue) were predicted within fluvial channel facies (yellow). The third track contains the edited and corrected predictions that were used later in the modeling stage.

3.3 Layering and Mapping

Conventionally, Safaniya member is divided into nine sequence stratigraphic zones. Each one represents a phase of delta development (Figure 11). The lower most three zones (6, 7 and 8) represent the bay and shallow marine deposits followed by three zones (3, 4 and 5) in which progradation of thick deltaic sands have occurred. Zone 2 was mainly deposited in a delta plain and marks the onset of delta retrograding towards the land. On top of all, Zone 1 was deposited marking the abandonment of delta (Chevron, 1990).

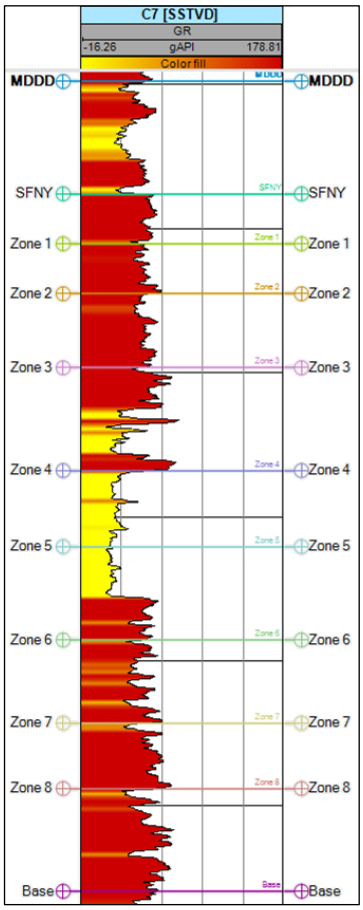

Figure 13 Eight markers are used to subdivide Safaniya member into nine zones and were assigned based on the geologic study by chevron.

The nine zones were mapped in Petrel using the original seismic surface of Mauddud member. The surface was first adjusted to well data and then isochores were constructed to map the underling zones by using the industry standard mapping algorithm "Convergent". The area of interest (AOI) was limited to the northern part of the field and did not cover the whole field because the used computer resources (mainly Random Access Memory) were not sufficient to handle the geologic model construction in the next phase of this study (Figure 12).

Layering helps to divide a geologic unit into several zones with each zone having different characteristics from the other such as: relative time of deposition, lithology, porosity, and permeability. Modeling layers with similar characteristics reduces the uncertainty and makes the used algorithm to work better since it will be dealing with conditional and narrower heterogeneity (Figure 13).

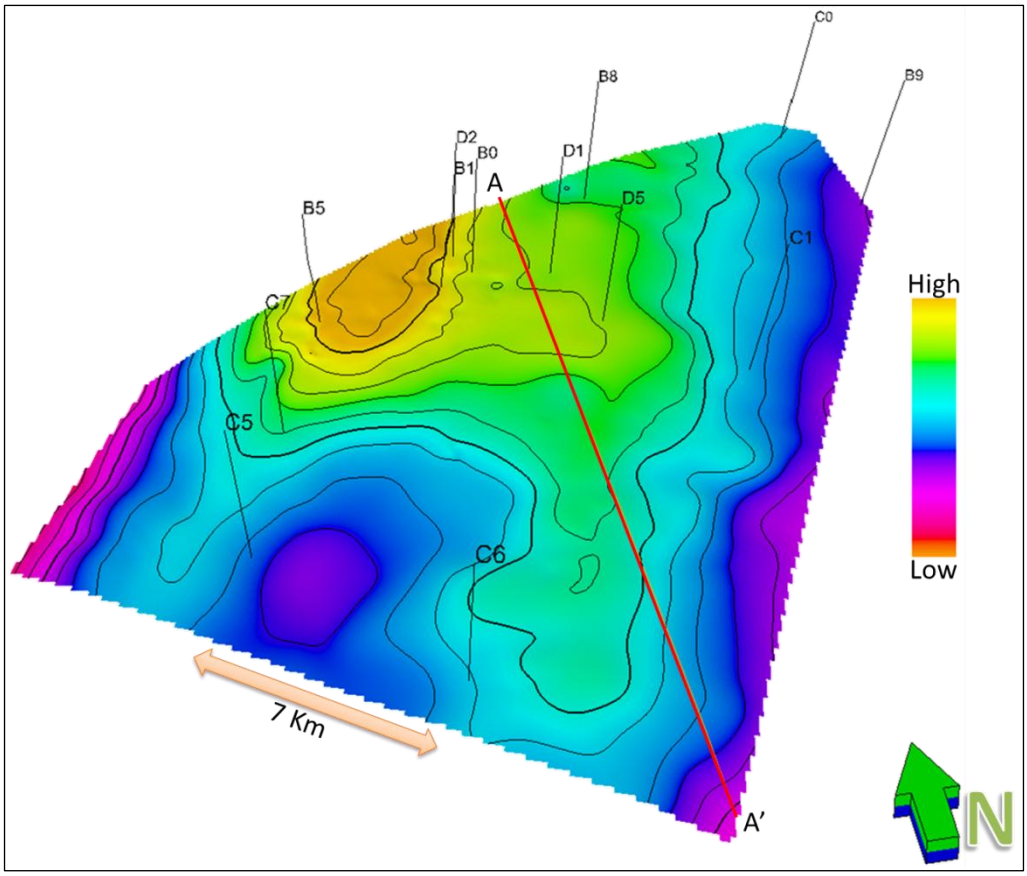

Figure 14 a 3D view of the upper most mapped structure "top of Mauddud member" using seismic combined with well control of the northern part of the field, a cross section that cuts the structure from north to south is also shown.

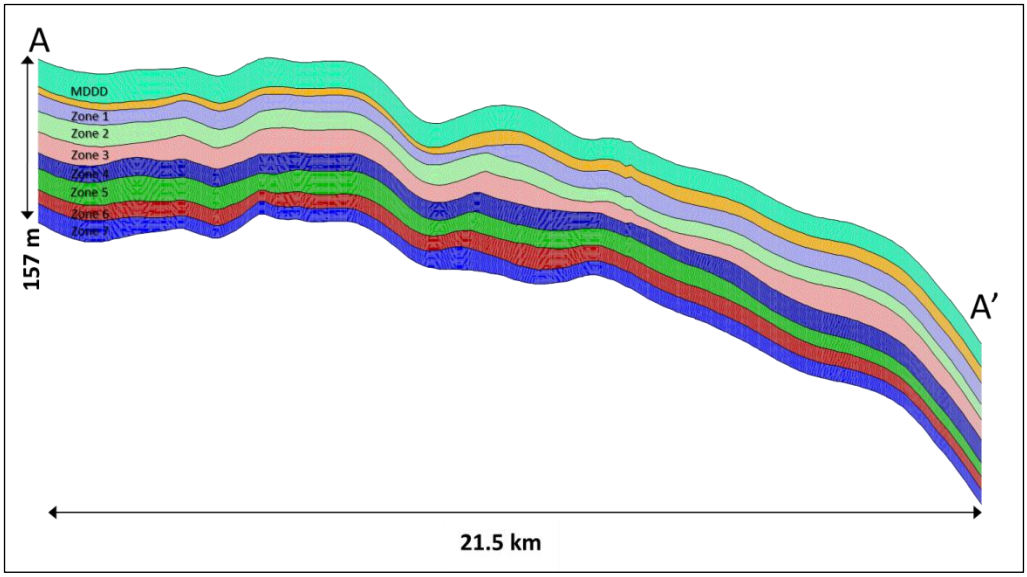

Figure 15 A cross section cutting the field from north (A) to south (A') showing the nine mapped zones from Mauddud on the top to Zone 7 at the bottom.

3.4 Conceptual Model

The conceptual model used in this research was based on the most recent sequence stratigraphic study performed on Safaniya member cores. The model basically is a fluvial dominated delta that has a sediment source in the southwest and prograding toward the northeast direction. The delta is similar to the Modern Highstand Fly river delta in Papua New Guinea (approximately 100 km in length and 60 km in width; Figure 14) in terms of sedimentary processes and facies distribution (Soliman, 2009). It mainly consists of three main parts:

- Lower stringers that were deposited in highstand systems tract (HST) and consists mainly of mouth bar facies associations
- Main sand that were deposited in falling stage systems tract (FSST) and consists mainly of braided fluvial, tidally-influenced fluvial and tidal bar facies associations
- Upper stringers that were deposited in transgressive systems tract (TST) and consists mainly of braided fluvial, tidally influenced fluvial, fluvial-tidal channel, muddy estuarine and tidal bar facies associations

The clastic sediment supply source was closer in the southern part of the field and the sandstone was deposited during a highstand and transgressive systems tract. Moving toward the north-northeast; deposits from the falling stage systems tract start to appear in the central part of the field. The northeastern most part of the field is the deepest, and there are deposits of lowstand systems tract (Figures 15 and 16).

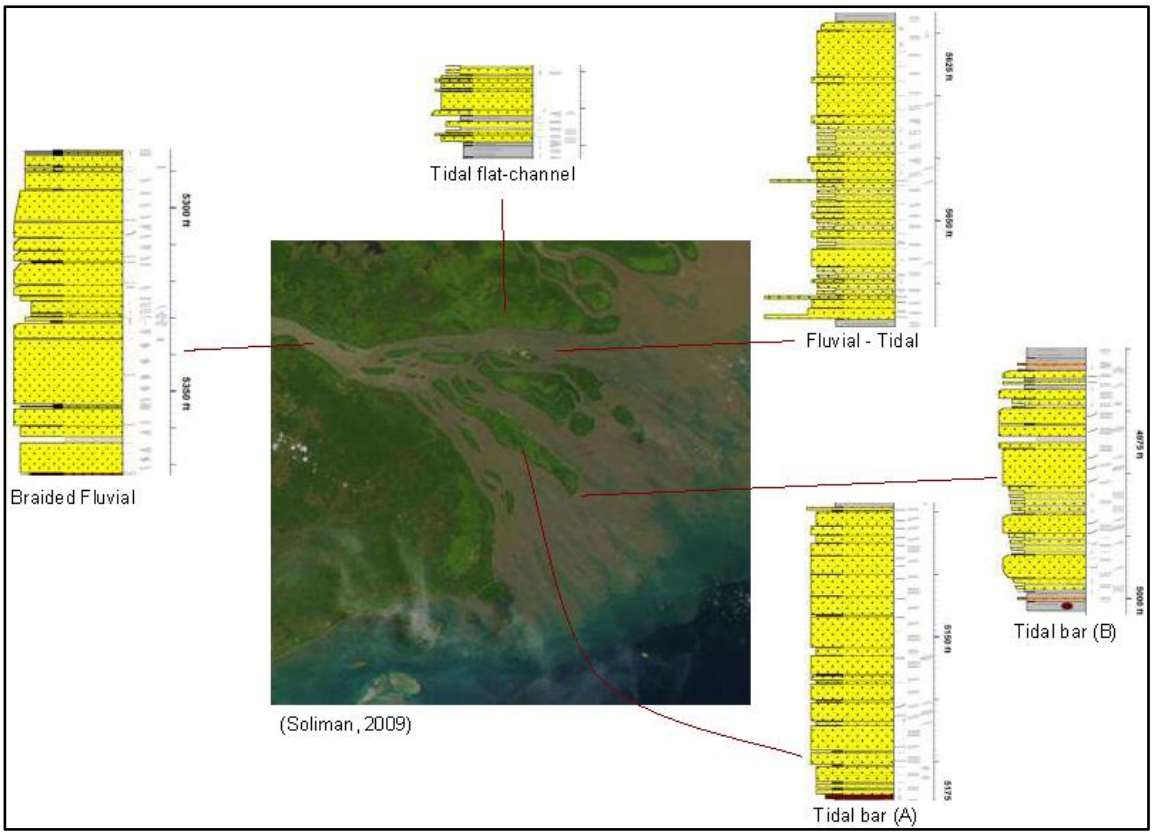

Figure 16 Relative distribution of the facies associations of the Safaniya Member compared the Modern Fly River delta. Note that the Fluvial-Tidal Facies Association is related to the largely abandoned northern distributary system of the Fly delta. The Tidal Bar Facies Association (A) is coarser grained and displays less well developed upward coarsening grain size trend than the distal equivalent of the Tidal Bar Facies Association (B) (Soliman, 2009).

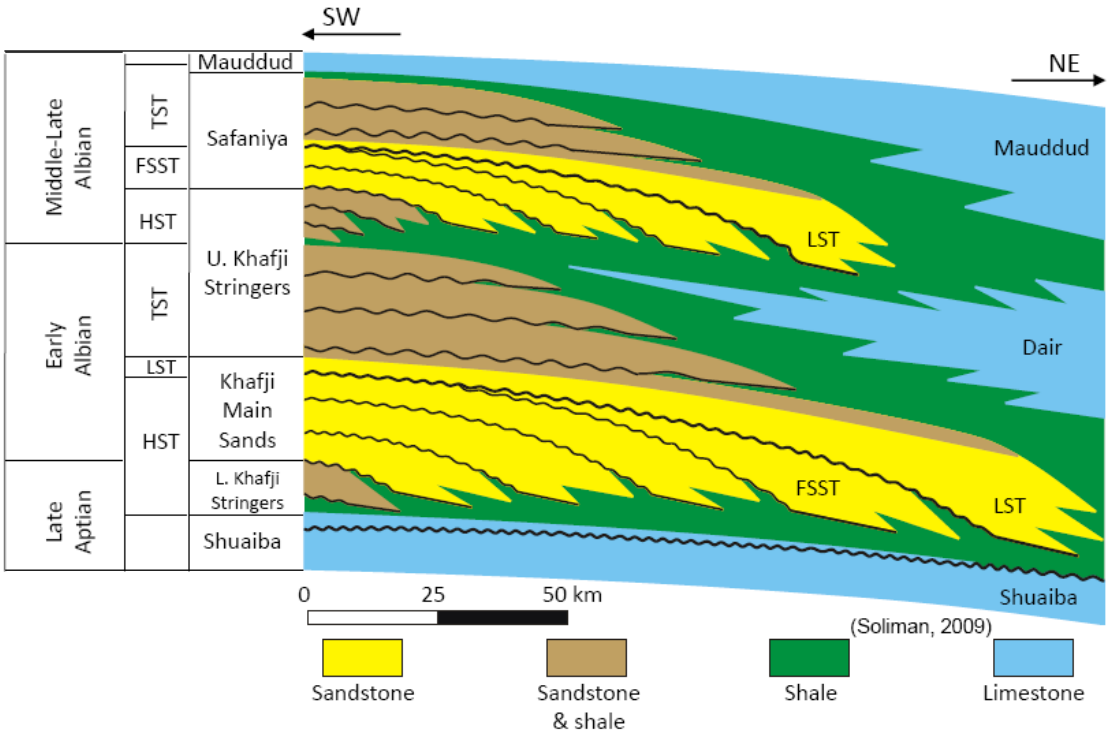

Figure 17 Stratigraphy of the Khafji and Safaniya Members. The Safaniya Member includes the Lower Safaniya Stringers, the Safaniya Main Sands and the Upper Safaniya Stringers (Soliman, 2009).

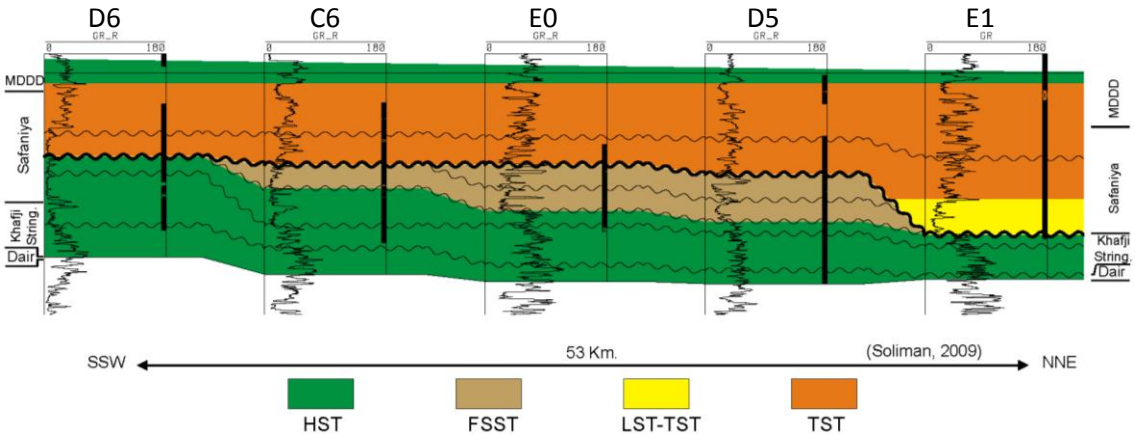

Figure 18 Sequence Stratigraphy of the Safaniya Member, Saudi Arabia (modified from Soliman, 2009). HST: Highstand Systems Tract, LST: Lowstand Systems Tract, TST: Trasgrissive Systems Tract, FSST: Falling Stage Systems Tract.

CHAPTER 4

MODELING STUDY & RISK ANALYSIS

4.1 Building 3D Model

Building the 3D structural model is the first step before performing any property modeling task. The model area of interest (AOI) is limited to the northern part of the field because of logistic reasons. One of them is that the model has to have large details and large resolution, and the existing computational facility is still limited in that respect.

The top of the model is Mauddud structural grid and the base is top of zone 8 (or interchangeably base of zone 7). In between these grids, nine zones were defined with no faults incorporated due to lack of accurate faults displacement interpretation from seismic profiles. The layers were depth adjusted to fit the 232 wells (13 cored, 188 non-cored and 31 blind-testing wells). The blind test wells were used at this stage to adjust the layers depths only. The cell size was designed as 125mX125m and the cell thickness was chosen to be 2ft in average. The reason for that cell size design was to preserve as much

sedimentological and structural data observed at well location as possible. With the large well density in this model; larger cell size might upscale these data and would produce unrealistic geological model. The model was rotated to N20E to be aligned with the field structure. The total number of cells in the 3D model was 23,456,540 which is considered as a large model to be constructed in a PC platform.

Property modeling is usually applied to specific zones and regions. If kriging is utilized, each grid cell will have a single value for each estimated property. However, simulations generate several realizations for each cell. As the grid cells often are much larger than the sample density for well logs, the available practical alternative is that well log data must be scaled up before they can be entered into the grid. The upscaling of facies log was performed on all 209 wells used in facies modeling (13 cored wells plus 188 non-cored). The averaging method used in this process is "most abundant facies", which selects the discrete value with the most occurrences in the log for each cell (Figure 17).

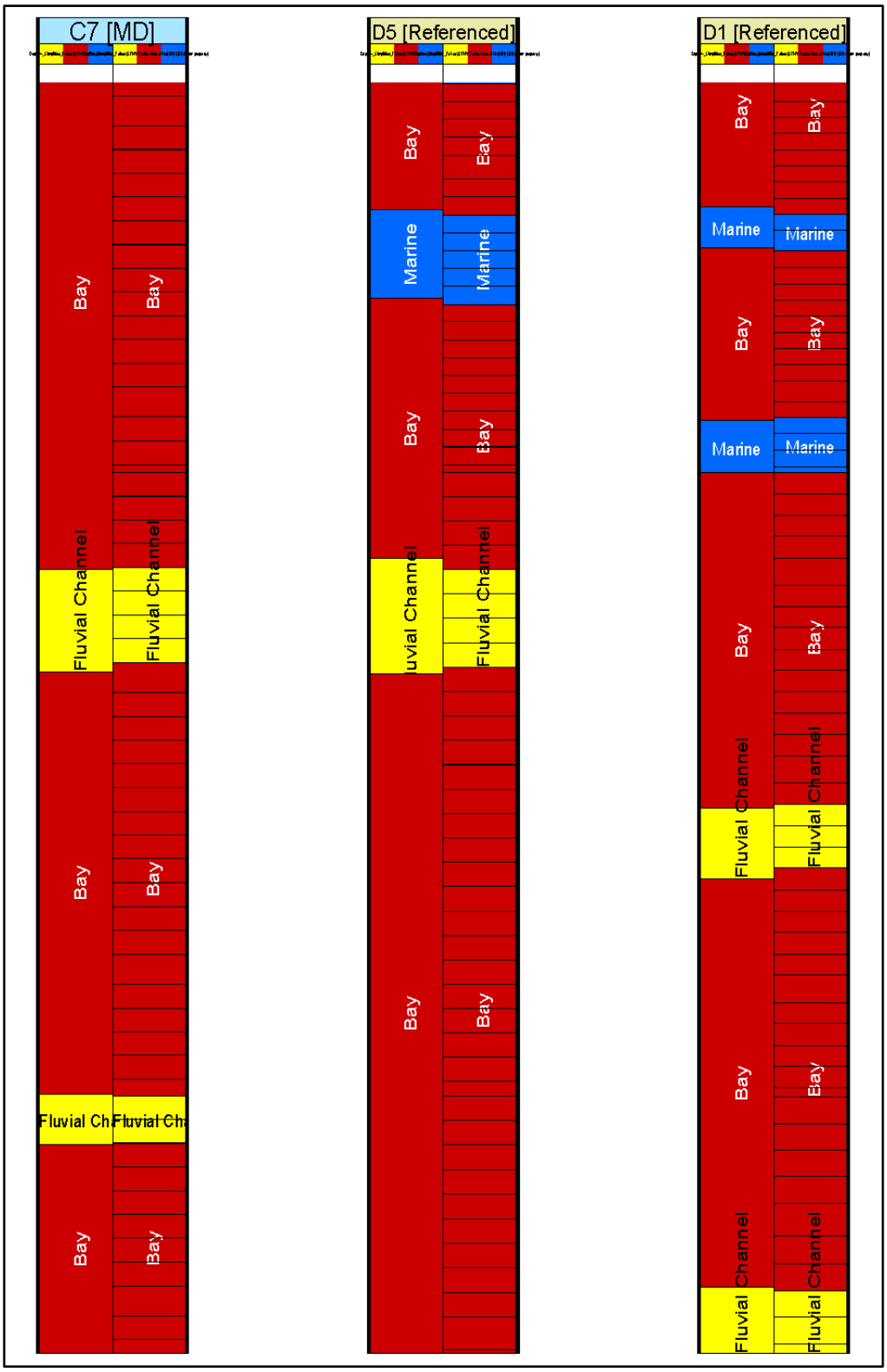

Figure 19 Three wells displaying the original facies log (on left) and the same log after upscaling (on right) where the value of the cell was assigned based on the value that is more represented in the cell interval.

The global fraction (or percentage) of each individual facies in each zone were derived from the upscaled log which is the default setting in Petrel. Any facies in any zone that is less than 1% is considered insignificant and simply was not modeled (Table 3).

Zone	Fluvial Channel	Bay	Marine	Total
MDDD	0.08%	33.95%	65.97%	100.00%
SFNY	1.18%	93.41%	5.41%	100.00%
Zone 1	6.28%	76.97%	16.75%	100.00%
Zone 2	20.02%	78.97%	1.01%	100.00%
Zone 3	44.59%	55.24%	0.17%	100.00%
Zone 4	71.75%	28.25%	0.00%	100.00%
Zone 5	60.29%	39.71%	0.00%	100.00%
Zone 6	22.64%	77.36%	0.00%	100.00%
Zone 7	13.17%	86.71%	0.12%	100.00%

Modeled
Not Modeled

Table 3 The percentages of each facies as derived from the upscaled facies logs in each geological zone, the facies that constitute less than 1% of the total volume of any zone was not modeled.

4.2 Pixel Based Models

4.2.1 Indicator Kriging Model

As mentioned in section 2.2.1, Indicator Kriging is a deterministic approach for modeling categorical properties such as facies. The outcome depends upon: the amount of data in each neighborhood, upscaling of cells, defined semi-variogram and the fraction of each individual facies. The advantage of using indicator kriging is that the results are repeatable, only resulting in a single realization,- and it avoids over interpretation of data.

The indicator kriging provides a minimum error-variance estimate and it tends to smooth the details and extreme values of the original set of data. This method should be used with caution because the results can be biased towards the dominant fraction from the global input data (Deutsch and Journel, 1998; Isaaks and Srivastava, 1989; Goovaerts, 1997).

Ordinary kriging was favored over simple kriging because it gives better results by re-estimating the mean at each location whereas the simple kriging just assumes a global mean. Spherical semi-variogram type was also favored over exponential and Gaussian because its smoothing effect is in between the other two types. Details about IK are shown in Appendix C.

To build a reliable IK model, semi-variogram parameters should be selected carefully. There are six main parameters that influence semi-variogram model which are used to guide the weighting in the 3D model (Figure 18):

- The **major range** that should be always larger than the average spacing of data points or at least larger than the data points minimum distance to avoid "bulls eye" effect and to provide structural connectivity.
- The **minor range** which is by default 90 degrees perpendicular to the major range and it should be less than anisotropy or equal to the isotropy value of the major range.
- The **azimuth** that defines depositional (or facies continuity) direction according to the conceptual model and if sat correct the result will be more geologically meaningful.

- The **vertical range** where the program searches for sample pairs vertically using the vertical search radius. This parameter should be selected according to the average geological layers thickness of the same properties.
- The **sill** is where the variogram flatten off or more practically equal-weighted variance of the data that is entered into semi-variogram calculation.
- The **nugget effect** is the discontinuity an the origin of the semi-variogram and ideally it should not exceed 30%.

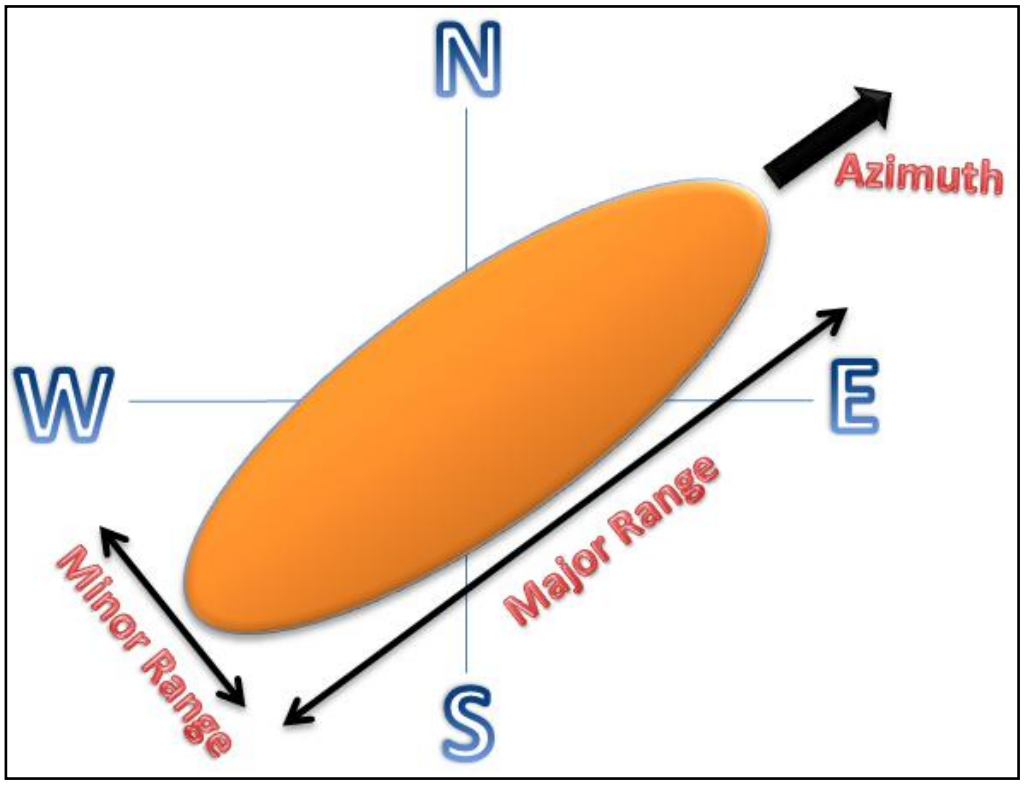

Figure 20 A diagram of the main three parameters that influence the semi-variogram model: major range, minor range, and azimuth. The fourth parameter, vertical range, is perpendicular to the page.

The approach that was implemented to identify the optimum values of the four semi-variogram parameters while building the model using indicator kriging algorithm is based on trial and error and systematically experimenting several semi-variograms until the 3D model becomes satisfying from geological point of view and provides high prediction success (Dubrule, 1998; Armstrong, 1998; Gilgen, 2006). The assumption made in this approach is that all the Safaniya member zones are having same semi-variogram parameters since it was noticed from Chevron (1990) and Soliman (2009) core studies that all the Safaniya zones have a common continuity direction which is N60E. The objective for calculating the semi-variogram is to reveal the geological trends in the data and this has been achieved through core studies and regional geological trends. Three examples for semi-variogram calculated for Safaniya member (all zones combined together in one semi-variogram) are shown in Appendix D. Figures A.D1 and A.D2 in Appendix D demonstrate the first attempts to best fit the semi-variograms exponential models. It resulted in 67.7% and 67.9% predictions success respectively. Spherical and Gaussian models could not be fitted with acceptable nugget effect values. Figure A.D3 in same appendix shows the best case that was achieved using indicator kriging technique which will be discussed in the remaining of this section that follows.

The trial and error approach was done by fixing the values of three parameters and then changing the value of the fourth parameter and run the model. The value that gives the best prediction will be then fixed and another parameter will be selected and have its value changed. This approach will provide the optimum value for each parameter and when all parameters were analyzed the combination of their best values should result in a model that gives the best prediction and the lowest uncertainty. Certainly, there might be

other factors that might affect the model predictability such as the layering scheme used in the model, the accuracy of core interpretation, the density of well control available in the model or it could be anything else. However, this approach focus only on the algorithm being used in Petrel, its parameters, and it assumes the other factors are good.

To commence this process, the semi-variogram parameters were set as following: Major Range at 6,000 m, Minor Range at 2,500 m, Vertical Range at 25 ft and Azimuth at 10 degrees. These values were selected based on the field's observations at wells. All zones were modeled with same parameters every time. Details of parameters selection are discussed below.

The first parameter that was selected is the azimuth because the orientation of geological bodies is apparently the most important factor for the purpose of this research. For example river channel always has a direction in the big scale even if it is locally changing. The values that were tested started from 10 degrees (from north) and were incremented by 10 until 180 degrees was reached. Each run took about an hour time to be completed and after each run the produced model was blind tested by using thirty four wells that were randomly selected for this purpose.

After completing all the eighteen runs, the results showed the best prediction occurred at 60 degrees azimuth with (74.7%) success, while the lowest prediction (73.0%) was obtained at 130 degrees azimuth. There was no significant difference between the lowest and highest predictions which was only 1.70%. Overall, the best obtained between the azimuths of 50 and 80 degrees which agrees with previously gained geological

knowledge about the source of the delta and its geographic orientation. This result came to confirm that the delta direction was northeast (Figure 19 & Table 4).

Testing the semi-variogram major range started from 2,500 m and increased by 1,500 m every other time until reaching the value of 16,000 m. These values were based on the geological understanding of the area that showed lateral continuity of sand bodies between offshore drilling platforms (about 2,500 m apart). Based on sequence stratigraphy, sand bodies could be laterally continuous even more than 15,000 m in the main sand zones. One aspect noticed while running the model was that every time the major range increases, the processing time required to complete the process increases. This continues until it reaches about one and half hour due to the inclusion of more data points in the estimation procedure. There was no significant difference between the lowest and highest predictions which was only 1.10%. The best prediction (74.7%) was given when using a major range of 6,500 m and the lowest prediction (73.6%) was obtained at a major range of 14,500 m (Figure 20 & Table 4).

The minor range testing started from 600 m and was incremented by 600 m until 6,000 m was reached. Although the difference between the highest (74.7%) and lowest (73.5%) predictions was negligible, there was a clear trend of enhancement of predictability as the minor range was increased. However, from minor range 2,500 m onward, the predictability seems to be stable. This might propose that minimum sand body's width averages around 2,500 m (Figure 21 & Table 4).

Vertical range values were tested starting from 5 ft to 50 ft, which is the average zone thickness of Safaniya member. An increment of 5 ft was applied when changing the

vertical range value. Results showed no trend and the best prediction was given when vertical range of 25 ft was tested. The difference between highest and lowest predictions was negligible and was only 0.7% (Figure 22 & Table 4). The reason for that small difference might be due to the fact that the whole vertical profile of Safaniya member was included while testing the vertical range values. Different results could be obtained if the vertical range of each zone of Safaniya member was tested individually.

The value that gave best prediction from each parameter was selected to build the final semi-variogram and IK models which generated prediction success of 74.7%.

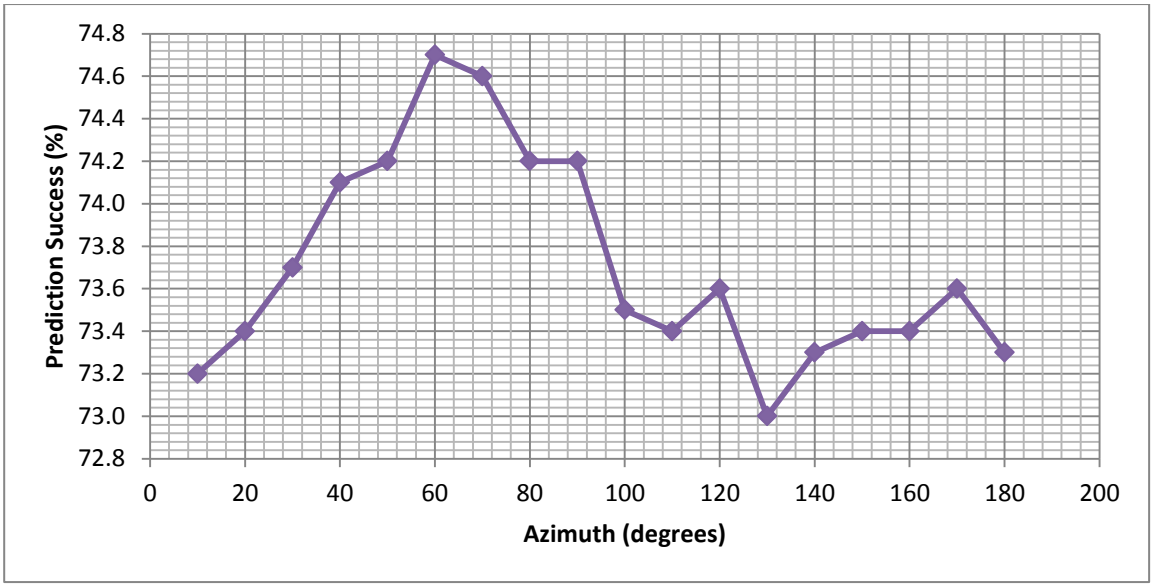

Figure 21 Tested semi-variogram azimuth values showed clearly that the prediction success is better between 50 and 80 degrees with the best prediction at 60 degrees.

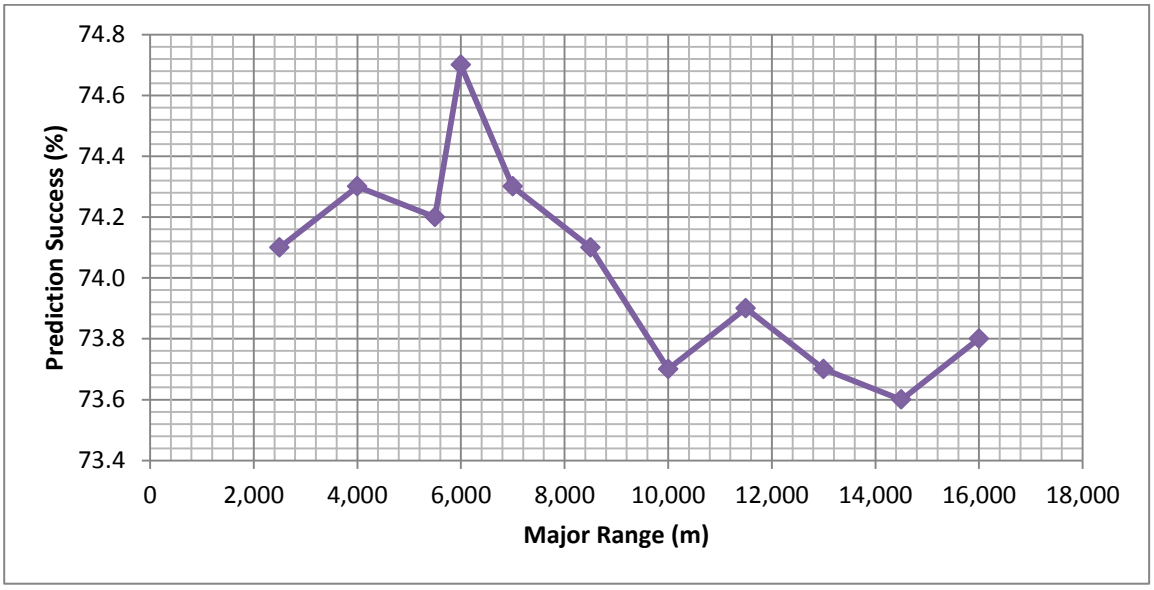

Figure 22 Tested semi-variogram major range values showed that the prediction success is butter between 2,500 and 8,500 m with the best prediction at 6,000 m.

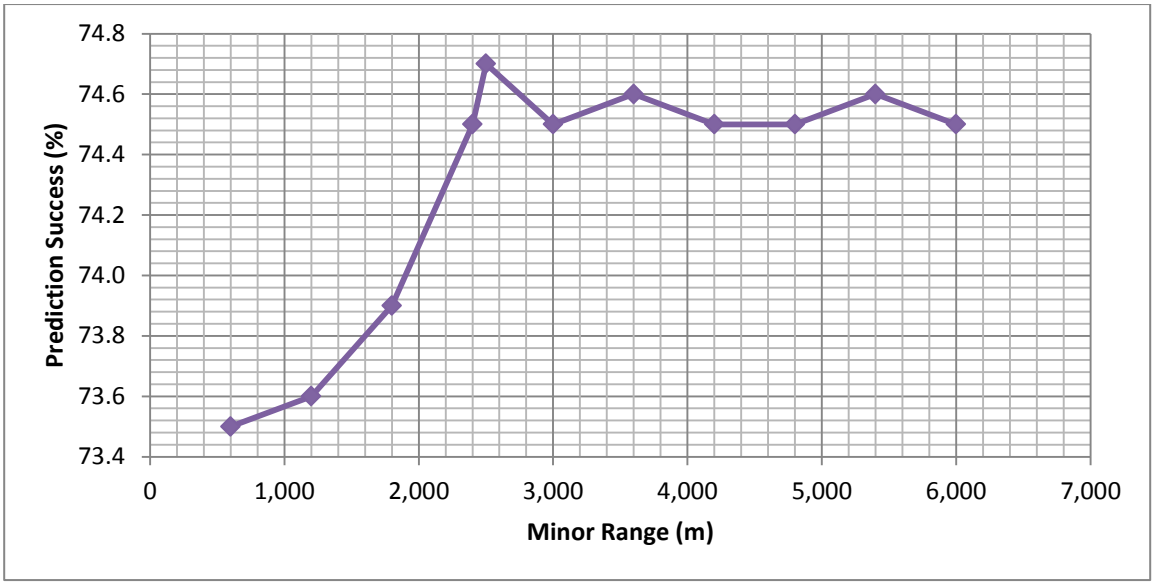

Figure 23 Tested semi-variogram minor range values showed a very clear trend of predictability enhancement as the value increased until 2,500 m after which the increase in minor range has no effect.

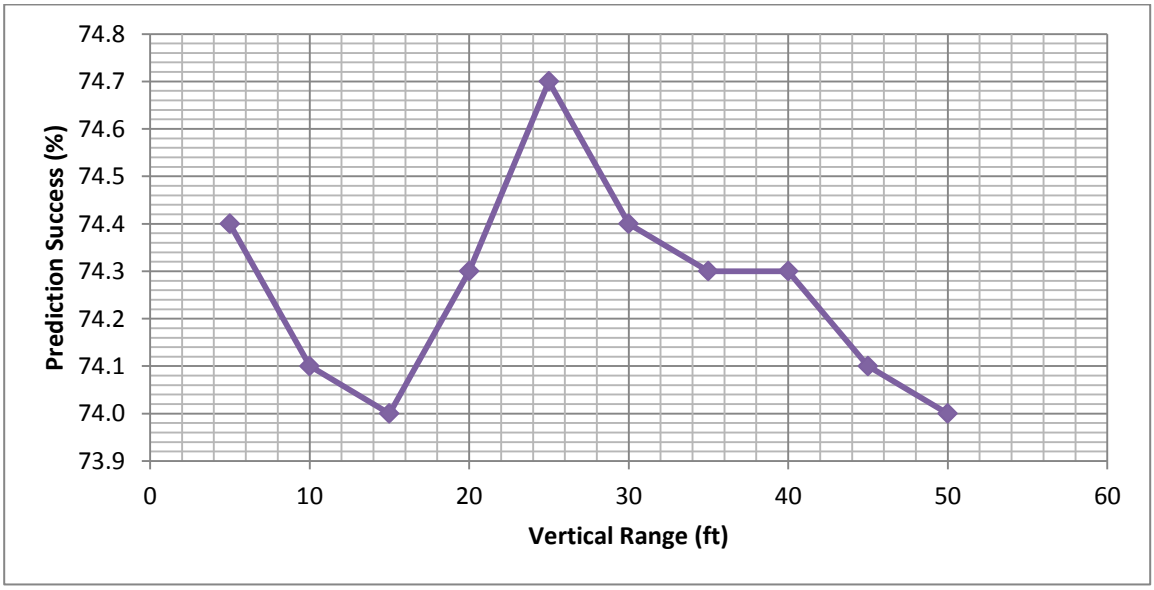

Figure 24 Tested semi-variogram vertical range values showed no clear trend since the difference between the highest and lowest prediction successes is only about 0.7%.

Risk Analysis for Indicator Kriging					
Major Dir Range, m	Minor Dir Range, m	Vertical Range, ft	Azimuth, deg	Prediction %	Error %
6,000	2,500	25	10	73.2	26.8
6,000	2,500	25	20	73.4	26.6
6,000	2,500	25	30	73.7	26.3
6,000	2,500	25	40	74.1	25.9
6,000	2,500	25	50	74.2	25.8
6,000	2,500	25	60	74.7	25.3
6,000	2,500	25	70	74.6	25.4
6,000	2,500	25	80	74.2	25.8
6,000	2,500	25	90	74.2	25.8
6,000	2,500	25	100	73.5	26.5
6,000	2,500	25	110	73.4	26.6
6,000	2,500	25	120	73.6	26.4
6,000	2,500	25	130	73.0	27.0
6,000	2,500	25	140	73.3	26.7
6,000	2,500	25	150	73.4	26.6
6,000	2,500	25	160	73.4	26.6
6,000	2,500	25	170	73.6	26.4
6,000	2,500	25	180	73.3	26.7
2,500	2,500	25	60	74.1	25.9
4,000	2,500	25	60	74.3	25.7
5,500	2,500	25	60	74.2	25.8
6,000	2,500	25	60	74.7	25.3
7,000	2,500	25	60	74.3	25.7
8,500	2,500	25	60	74.1	25.9
10,000	2,500	25	60	73.7	26.3
11,500	2,500	25	60	73.9	26.1
13,000	2,500	25	60	73.7	26.3
14,500	2,500	25	60	73.6	26.4
16,000	2,500	25	60	73.8	26.2
6,000	600	25	60	73.5	26.5
6,000	1,200	25	60	73.6	26.4
6,000	1,800	25	60	73.9	26.1
6,000	2,400	25	60	74.5	25.5
6,000	2,500	25	60	74.7	25.3
6,000	3,000	25	60	74.5	25.5
6,000	3,600	25	60	74.6	25.4
6,000	4,200	25	60	74.5	25.5
6,000	4,800	25	60	74.5	25.5
6,000	5,400	25	60	74.6	25.4
6,000	6,000	25	60	74.5	25.5
6,000	2,500	5	60	74.4	25.6
6,000	2,500	10	60	74.1	25.9
6,000	2,500	15	60	74.0	26.0
6,000	2,500	20	60	74.3	25.7
6,000	2,500	25	60	74.7	25.3
6,000	2,500	30	60	74.4	25.6
6,000	2,500	35	60	74.3	25.7
6,000	2,500	40	60	74.3	25.7
6,000	2,500	45	60	74.1	25.9
6,000	2,500	50	60	74.0	26.0
6,000	2,500	25	60	74.7	25.3

Tested Parameter **Best Prediction**

Table 4 Each semi-variogram parameter affecting the output indicator kriging model was tested using different values and the best value was fixed in the next tested parameter and finally the best values of each parameters were combines to build the final model.

Although the model built using indicator kriging model gave a good percentage of prediction success, the model did not visually look geologically correct in some cases. For example, in some zones such as zone 6 and zone 7 the sandstone bodies were scattered and not connected. This might be due to the nature of IK algorithm which connects the dominant facies in the modeled zones. This will result in connected shales in zones 1, 2, 6, and 7. The opposite is true for the other zones. Another observation is that some facies were visualized as straight line as the case in zone 5, Figure 23, but this could be purely a bug in the software's algorithm. The expected geometry of sandstone bodies cannot be reproduced by kriging, but the numerical results are good due to the large amount of data utilized. The model, however, kept the general conceptual model features such as having main sand bodies in zone 4 and zone 5 which were deposited during maximum progradation of the delta and then started to retrograde during the deposition of zone 3 and finally was capped by the limestone of Mauddud member during a maximum flooding event (Figures 24).

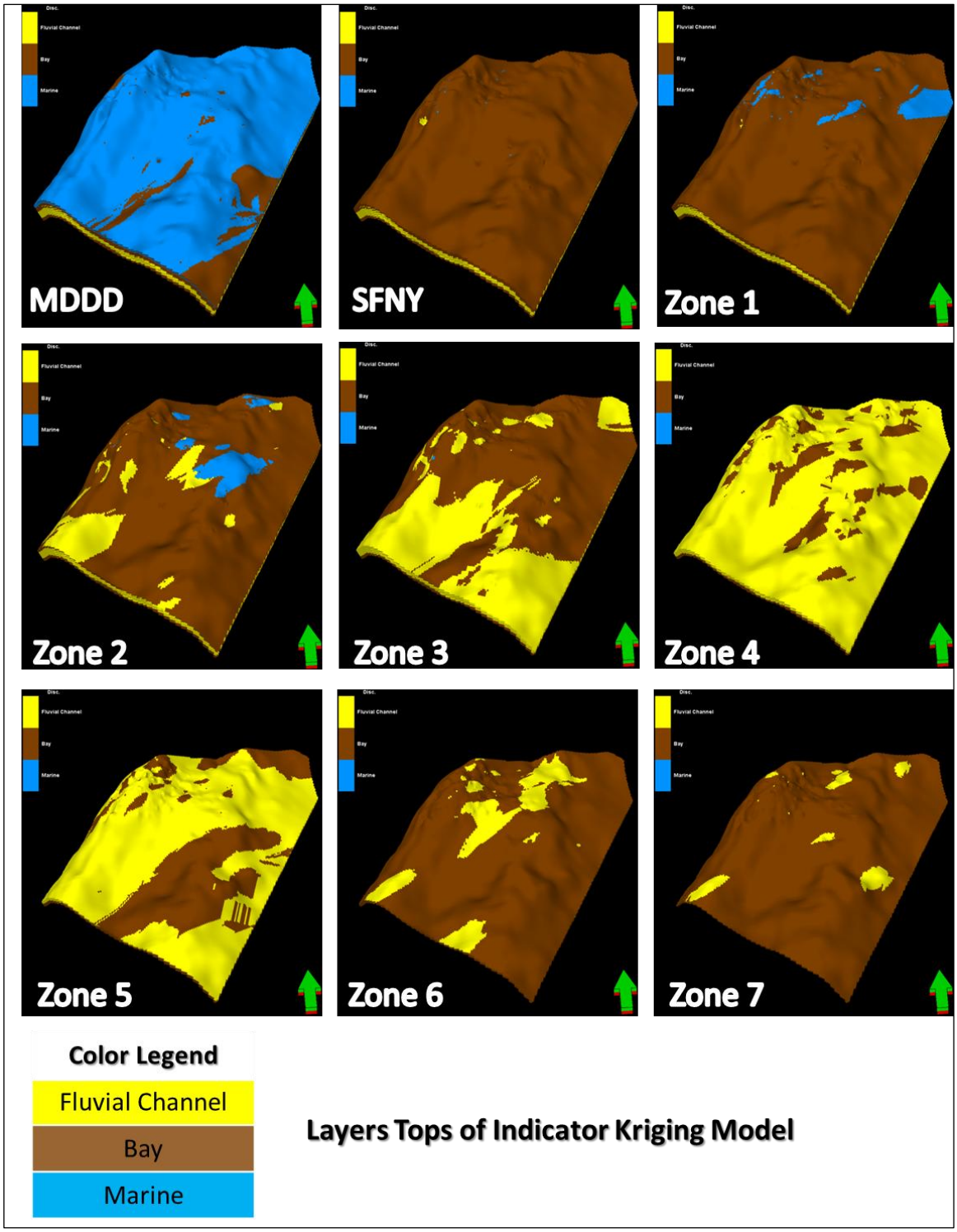

Figure 25 Top view of each modeled zone using indicator kriging algorithm. Main sand zones are 3, 4 and 5 whereas stringers zones are 2, 6 and 7.

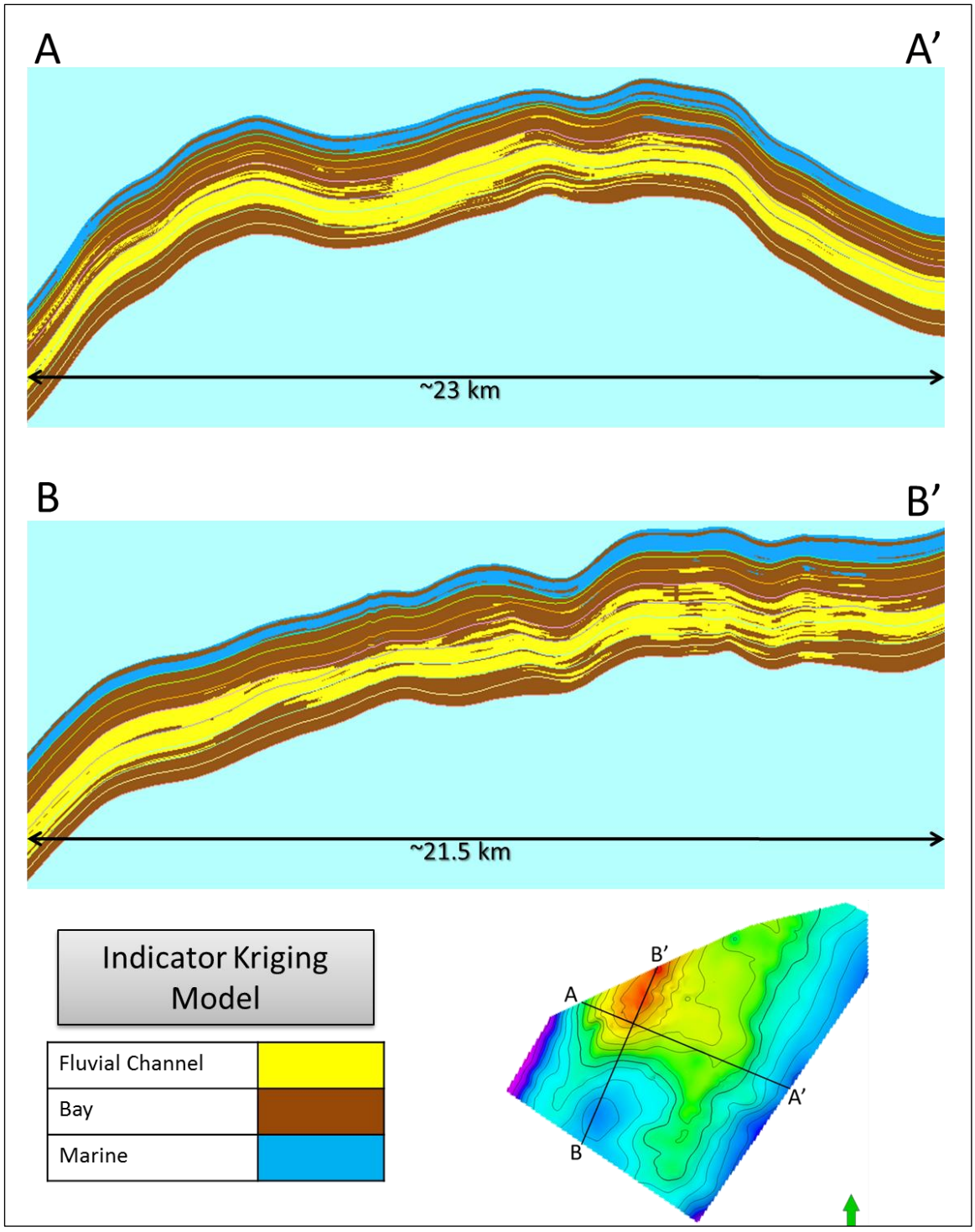

Figure 26 Two cross sections cutting across indicator kriging model where the facies look blocky and thin beds are not very well represented.

4.2.2 Sequential Indicator Simulation Model

Sequential indicator simulation (SIS) is the most appropriate algorithm to use when the shape of particular facies bodies is uncertain. A constraint for proper use of SIS is to have abundant data, and/or maps and trends that control the generated facies realizations. For example, if seismic attributes are used to control the probability of a sandstone and shale facies occurrence then SIS can use that information to provide valid constrained heterogeneity. The SIS method is stochastic, so whenever the seed number changes, different realizations will be generated (Hohn, 1998). The results are dependent upon: upscaled cells, the defined semi-variogram, random seed and the frequency distribution of upscaled data points. Details about SIS are discussed in Appendix E.

The previously-used semi-variogram parameters that gave the best prediction success in indicator kriging model were employed to build the sequential indicator simulation model and assumed to generate the best simulation success. Theoretically, infinite number of simulations can be generated; however, in this case study, eleven realizations using different seed number were created. Results showed slightly lower prediction success than the indicator kriging model averaging 67.7% (Table 5). The difference between the highest (68.8%) and lowest (67.1%) prediction was only 1.7%. One possible reason for the resulted low prediction might be due to the fact that more realizations are needed. Another reason could be related to the generalized semi-variogram model which was considering all the layers and data point. If the semi-variogram was computed for each zone independently then improved prediction is expected.

This algorithm, in contrast to Indicator Kriging, captures thin sedimentary beds which are represented better. This can be related to the facies log upscaling which was performed prior to distributing the facies between and outside well control (Figures 25 and 26).

Risk Analysis for Sequential Indicator Simulation							
Realization#	**Major Dir. Range, m**	**Minor Dir. Range, m**	**Vertical Range, ft**	**Azimuth, degrees**	**Prediction, %**	**Error, %**	**Notes**
1	6,000	2,500	25	60	67.3	32.7	average predictions of the ten realizations is 67.7%
2	6,000	2,500	25	60	67.1	32.9	
3	6,000	2,500	25	60	67.6	32.4	
4	6,000	2,500	25	60	67.7	32.3	
5	6,000	2,500	25	60	67.6	32.4	
6	6,000	2,500	25	60	68.0	32.0	
7	6,000	2,500	25	60	68.8	31.2	
8	6,000	2,500	25	60	68.1	31.9	
9	6,000	2,500	25	60	67.5	32.5	
10	6,000	2,500	25	60	67.7	32.3	
11	6,000	2,500	25	60	67.5	32.5	seed #9823

Table 5 The prediction success produced by eleven SIS model realizations showed slightly lower prediction percentages than indicator kriging model.

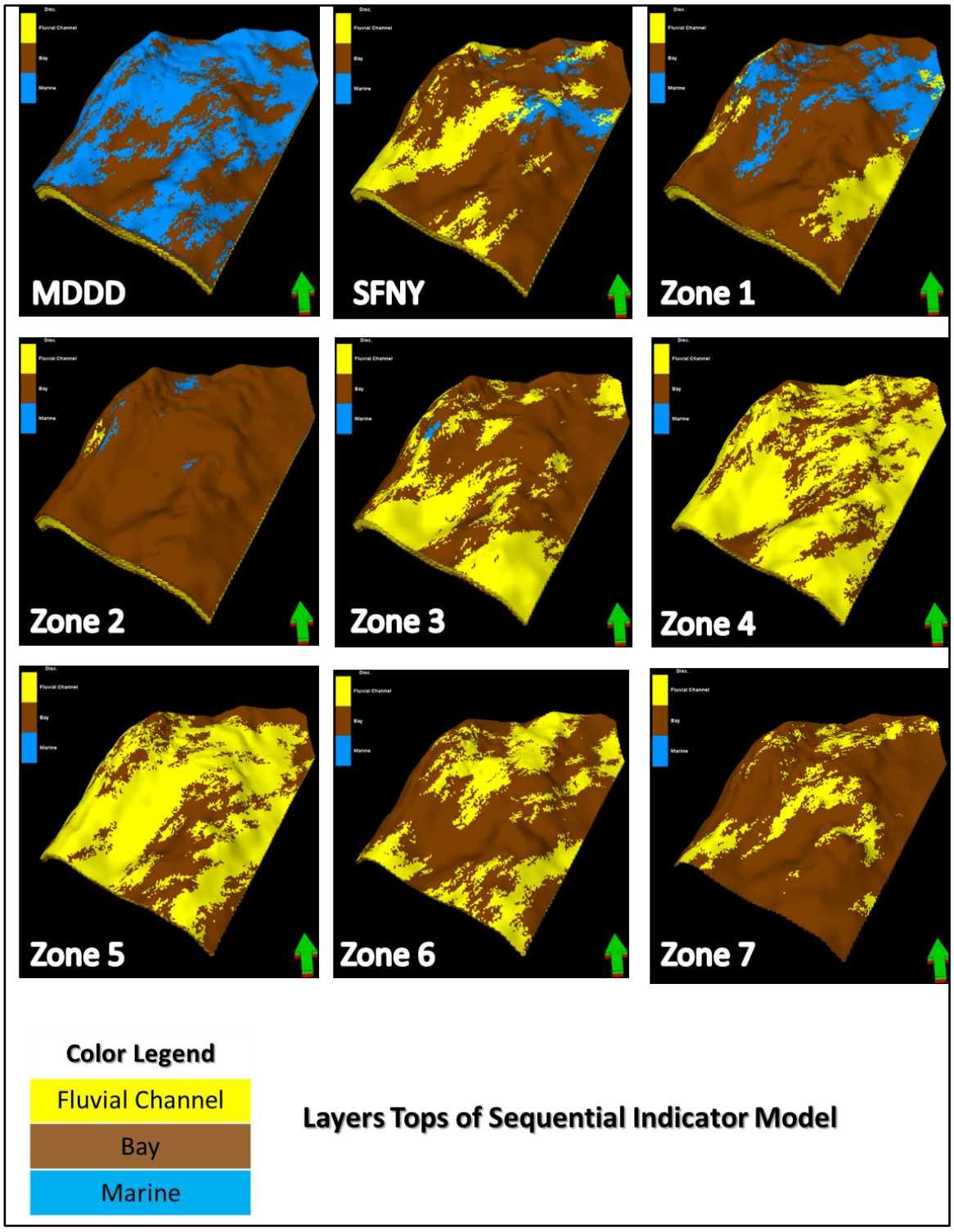

Figure 27 Top view of each modeled zone using sequential indicator simulation algorithm. Main sand zones are 3, 4 and 5 whereas stringers zones are 2, 6 and 7.

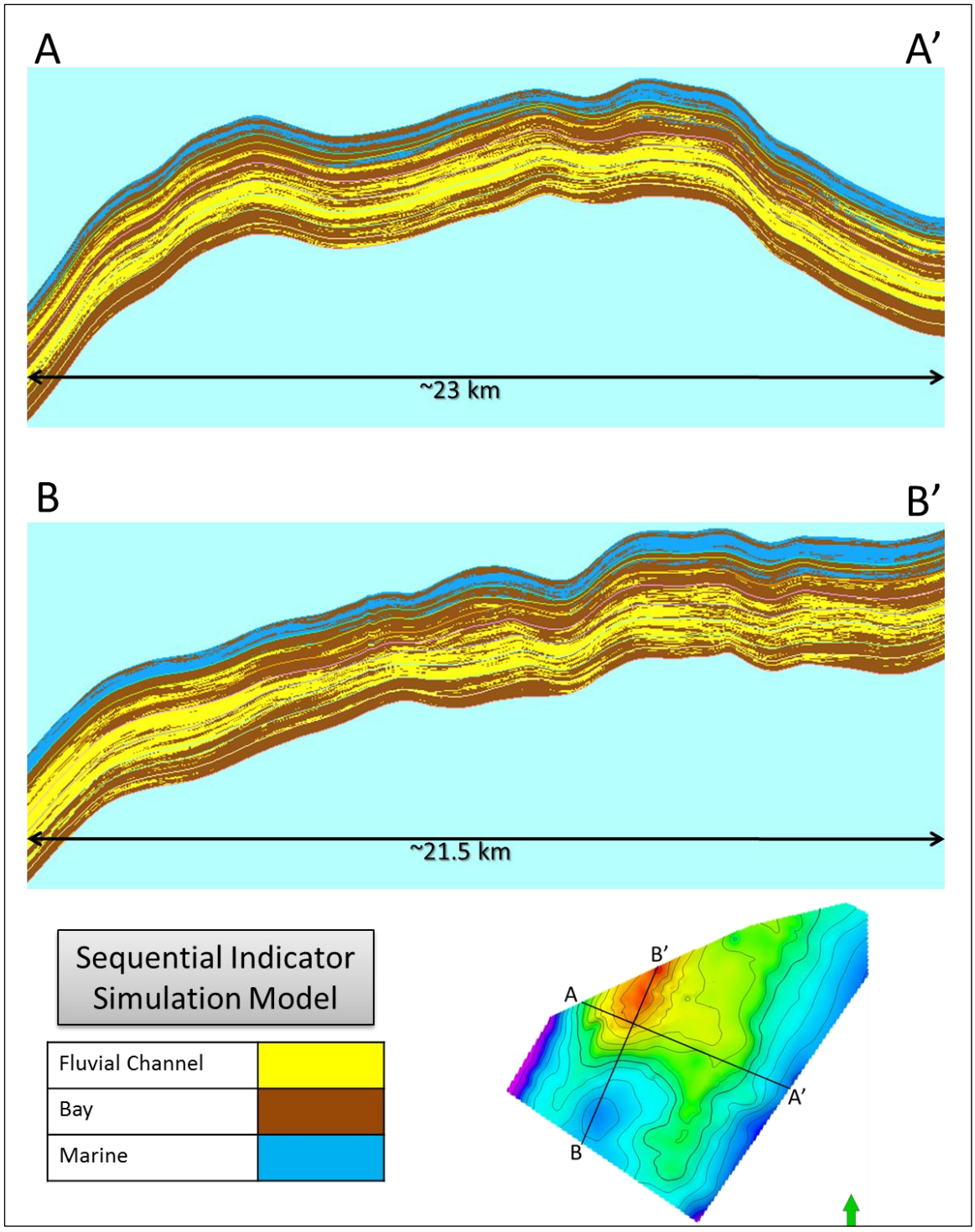

Figure 28 Two cross sections cutting across sequential indicator simulation model where the facies look less blocky than indictor kriging model and thin beds are represented better.

4.3 Object Based Model

Object Modeling allows populating a discrete facies model with objects which are generated and distributed stochastically. All geometrical inputs controlling the body shape (width/thickness, etc.) can either be defined deterministically, follow a defined statistical distribution or be assigned using a trend map. The background facies can be assigned a given facies code or an existing facies model (Brandsæter et al, 2001). Details about this approach are discussed in Appendix F.

After defining facies from cored wells; a Trial-and-Error approach was used to begin Object modeling. First, the parameters affecting the output model are defined as in Indicator Kriging approach. Second, each parameter is tested several times using different value. The value that gives highest prediction is then fixed and the next parameter is tested. Third, the fixed values of each parameter are then combined together to produce the final model. Finally, one has to produce several realizations. In this study, only four realizations were produced due to computing time limitation and to achieve the project objective on schedule.

Each category is generated by matching well data, then additional objects are inserted until the global fraction achieves the required proportion. Bodies can be inserted into wells as long as they are not conflicting with the surrounding well data (Qi et al, 2007).

In this case study, the three main facies to be modeled are: marine, fluvial channel and bay. The object selected for marine facies is the “rounded ellipse” because it is the geometrical object that seems to be adequate. Also, this object is used to cover a large

area which is a typical marine deposit feature. The object selected to model the channels is the sinuous "fluvial channel". Bay facies were considered as background facies and hence have no specific geometries.

The rounded ellipse object has four main controlling parameters: minor width, major to minor axes ratio, thickness and orientation. The fluvial channel object has five controlling parameters: amplitude, wavelength, width, thickness and orientation (Figure 27). Object orientation was considered as a common parameter between the two objects. All the parameters listed above were tested to check the model predictability (success to regenerated subsurface reality) using different values and the best values were fixed before testing the next parameter. The number of iterations performed on each parameter was limited to five as a maximum because it was taking around three to four hours to complete one run.

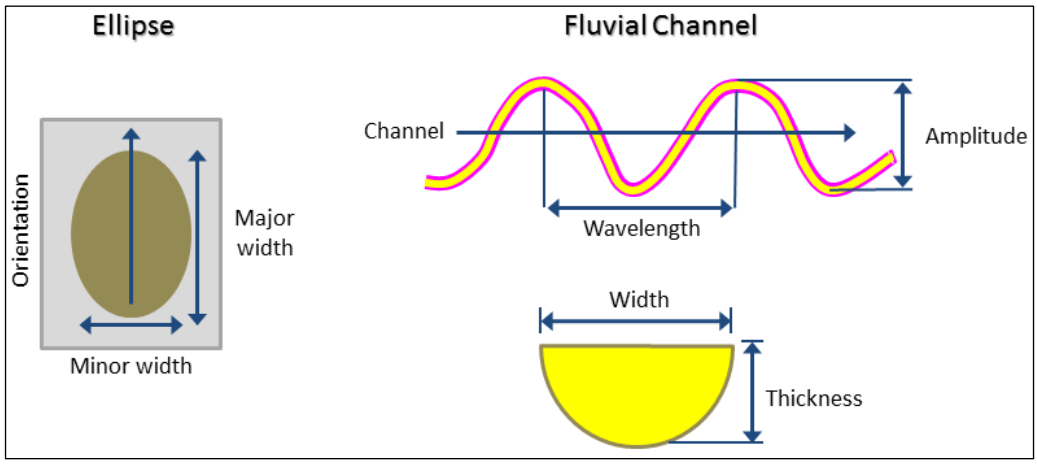

Figure 29 The different parameters affecting the output object model in both the ellipse and fluvial channel object (modified from Schlumberger, 2009).

Fluvial channel object was tested first by changing the width value and the results showed that this parameter has a minor effect on the object model predictability of about 1.5%. The same also applies to the orientation and wavelength parameters where the change in model predictability was around 1% and 1.2% respectively. However, the predictability was greatly influenced by channel amplitude and thickness parameters. It was noticed that when amplitude is increased; the predictability is also increasing up to 3.9%. This result supports the fact the fluvial channels of Safaniya reservoir were of the braided type. Unexpectedly, the object model predictability increased significantly as the channel thickness reduced. The predictability increased by 8.9% when average channel thickness was reduced from 50 to 2.5 feet. Core description showed that most sand channel thicknesses were ranging from 10 to 30 feet and it can be more than 50 feet in the main sand portion of the reservoir. This may indicate the presence of stacked channels. Therefore as the thickness at wells are greater than the object thickness; the algorithm can insert several objects on top of each other (Table 6).

Marine objects were experimented by varying its three parameters. As the case in fluvial channel objects; the main factor found to influence the predictability of the model is the thickness. The other two parameters, major and minor widths, did not affect the predictability by more than 0.7% (Table 6).

The resulted Safaniya clastics channels objects looked geologically acceptable from visual point of view. However, Mauddud carbonate objects did not look realistic and geologically acceptable because of their oval shape in the model. Even after increasing the lateral extension of these objects; the model did not look realistic because the carbonate ellipses were “randomly” scattered over the field and did not show a geological trend. The

channels, however, were geologically acceptable as sand distribution geometries but in all Safaniya member zones there is a feeling that there should be more channels especially in the main sand layers: zones 3, 4 and 5 (Figures 28 and 29). The object model was giving predictability of 65.3% at its best after combing all the best values for each parameter and running four realizations (Table 6).

Run #	Marine (Rounded Ellipse)								Channel (Fluvial Channel)														Prediction %	Error %
	Minor Width, m			Maj:Min			Thickness, ft		Orientation, deg			Amplitude, m			Wavelength, m			Width, m			Thickness, ft			
	Min	Med	Max	Min	Med	Max	Min	Med	Max	Min	Med	Max	Min	Med	Max	Min	Med	Max	Min	Med	Max	Min	Med	Max		
1	2,000	4,000	6,000	0.5	0.75	1	5	25	50	40	65	90	100	300	500	1,000	1,500	2,000	200	600	1,000	5	25	50	56.1	43.9
2	2,000	4,000	6,000	0.5	0.75	1	5	25	50	40	65	90	100	300	500	1,000	1,500	2,000	200	1,100	2,000	5	25	50	54.6	45.4
2	2,000	4,000	6,000	0.5	0.75	1	5	25	50	40	65	90	100	300	500	1,000	1,500	2,000	100	800	1,500	5	25	50	55.1	44.9
4	2,000	4,000	6,000	0.5	0.75	1	5	25	50	40	65	90	100	300	500	1,000	1,500	2,000	100	450	800	5	25	50	55.8	44.2
5	2,000	4,000	6,000	0.5	0.75	1	5	25	50	50	60	80	100	300	500	1,000	1,500	2,000	200	600	1,000	5	25	50	57.1	42.9
6	2,000	4,000	6,000	0.5	0.75	1	5	25	50	55	60	65	100	300	500	1,000	1,500	2,000	200	600	1,000	5	25	50	56.1	43.9
7	2,000	4,000	6,000	0.5	0.75	1	5	25	50	50	70	90	100	300	500	1,000	1,500	2,000	200	600	1,000	5	25	50	56.5	43.5
8	2,000	4,000	6,000	0.5	0.75	1	5	25	50	50	60	80	50	100	150	1,000	1,500	2,000	200	600	1,000	5	25	50	54.5	45.5
9	2,000	4,000	6,000	0.5	0.75	1	5	25	50	50	60	80	50	175	300	1,000	1,500	2,000	200	600	1,000	5	25	50	55.1	44.9
10	2,000	4,000	6,000	0.5	0.75	1	5	25	50	50	60	80	50	425	800	1,000	1,500	2,000	200	600	1,000	5	25	50	57.4	42.6
11	2,000	4,000	6,000	0.5	0.75	1	5	25	50	50	60	80	50	775	1,500	1,000	1,500	2,000	200	600	1,000	5	25	50	58.4	41.6
12	2,000	4,000	6,000	0.5	0.75	1	5	25	50	50	60	80	50	775	1,500	100	1,050	2,000	200	600	1,000	5	25	50	57.6	42.4
13	2,000	4,000	6,000	0.5	0.75	1	5	25	50	50	60	80	50	775	1,500	1,500	2,000	2,500	200	600	1,000	5	25	50	58.4	41.6
14	2,000	4,000	6,000	0.5	0.75	1	5	25	50	50	60	80	50	775	1,500	2,000	2,500	3,000	200	600	1,000	5	25	50	58.8	41.2
15	2,000	4,000	6,000	0.5	0.75	1	5	25	50	50	60	80	50	775	1,500	2,500	3,000	3,500	200	600	1,000	5	25	50	58.8	41.2
16	2,000	4,000	6,000	0.5	0.75	1	5	25	50	50	60	80	50	775	1,500	2,500	3,000	3,500	200	600	1,000	5	50	100	54.6	45.4
17	2,000	4,000	6,000	0.5	0.75	1	5	25	50	50	60	80	50	775	1,500	2,500	3,000	3,500	200	600	1,000	5	15	30	61.0	39.0
18	2,000	4,000	6,000	0.5	0.75	1	5	25	50	50	60	80	50	775	1,500	2,500	3,000	3,500	200	600	1,000	5	10	15	62.0	38.0
19	2,000	4,000	6,000	0.5	0.75	1	5	25	50	50	60	80	50	775	1,500	2,500	3,000	3,500	200	600	1,000	1	5	10	63.4	36.6
20	2,000	4,000	6,000	0.5	0.75	1	5	25	50	50	60	80	50	775	1,500	2,500	3,000	3,500	200	600	1,000	1	2.5	5	63.5	36.5
21	2,000	4,000	6,000	0.5	0.75	1	5	15	30	50	60	80	50	775	1,500	2,500	3,000	3,500	200	600	1,000	1	2.5	5	63.9	36.1
22	2,000	4,000	6,000	0.5	0.75	1	5	10	15	50	60	80	50	775	1,500	2,500	3,000	3,500	200	600	1,000	1	2.5	5	64.0	36.0
23	2,000	4,000	6,000	0.5	0.75	1	1	2.5	5	50	60	80	50	775	1,500	2,500	3,000	3,500	200	600	1,000	1	2.5	5	64.6	35.4
24	2,000	4,000	6,000	0.5	0.75	1	0.5	0.75	1	50	60	80	50	775	1,500	2,500	3,000	3,500	200	600	1,000	1	2.5	5	57.8	42.2
25	10,000	10,000	10,000	0.5	0.75	1	1	2.5	5	50	60	80	50	775	1,500	2,500	3,000	3,500	200	600	1,000	1	2.5	5	65.3	34.7
26	15,000	15,000	15,000	0.5	0.75	1	1	2.5	5	50	60	80	50	775	1,500	2,500	3,000	3,500	200	600	1,000	1	2.5	5	64.6	35.4
27	10,000	10,000	10,000	1	1	1	1	2.5	5	50	60	80	50	775	1,500	2,500	3,000	3,500	200	600	1,000	1	2.5	5	64.9	35.1
28	10,000	10,000	10,000	0.5	0.75	1	1	2.5	5	50	60	80	50	775	1,500	2,500	3,000	3,500	200	600	1,000	1	2.5	5	65.3	34.7
Three Realiz's	10,000	10,000	10,000	0.5	0.75	1	1	2.5	5	50	60	80	50	775	1,500	2,500	3,000	3,500	200	600	1,000	1	2.5	5	65.3	34.7
	10,000	10,000	10,000	0.5	0.75	1	1	2.5	5	50	60	80	50	775	1,500	2,500	3,000	3,500	200	600	1,000	1	2.5	5	64.9	35.1
	10,000	10,000	10,000	0.5	0.75	1	1	2.5	5	50	60	80	50	775	1,500	2,500	3,000	3,500	200	600	1,000	1	2.5	5	64.7	35.3

Tested Parameter

Best Prediction

Table 6 The prediction successes produced by thirty one object model realizations showed that the most influence is resulting from the thickness of both objects and the amplitude of the channel object.

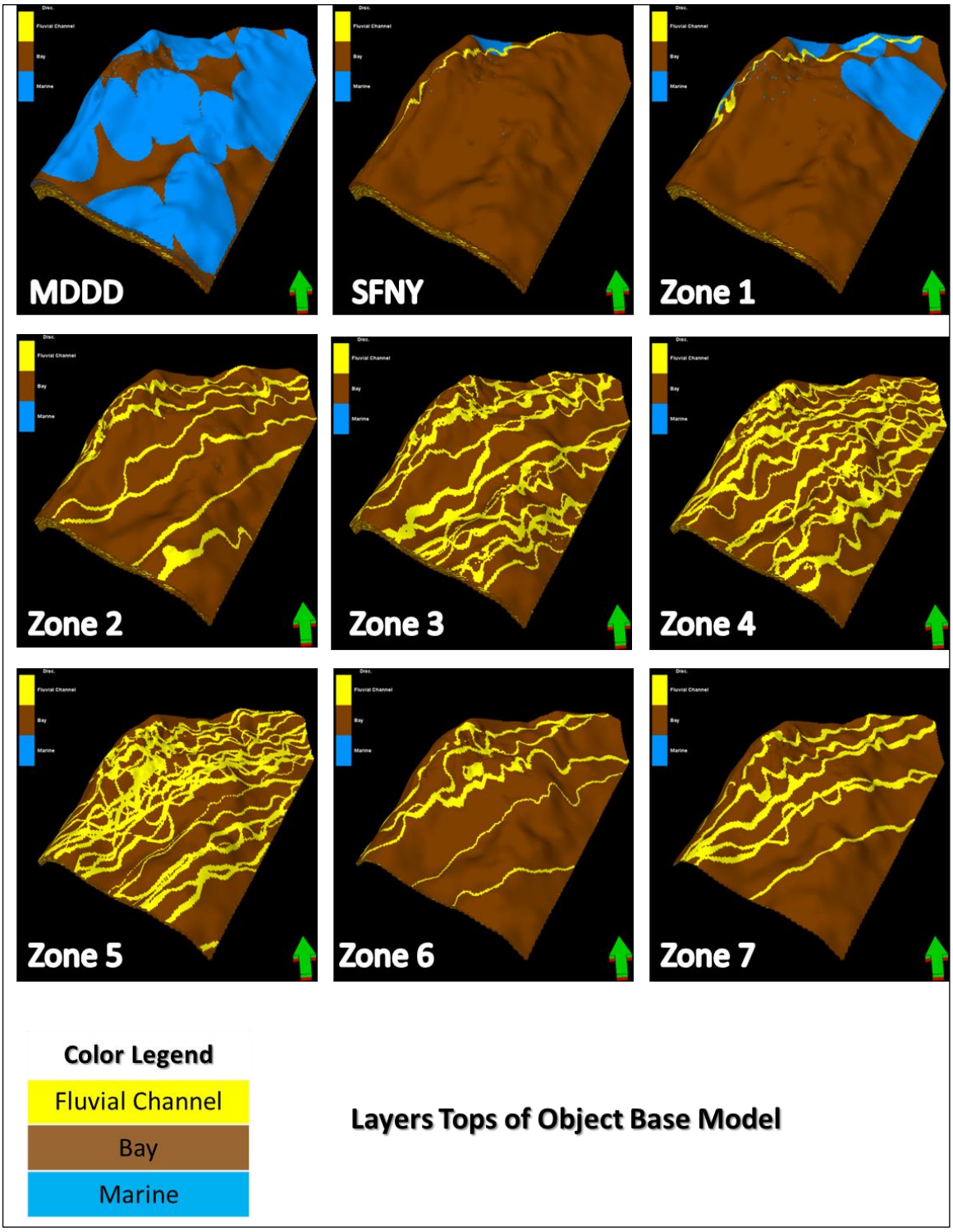

Figure 30 Top view of each modeled zone using object modeling method. Main sand zones are 3, 4 and 5 whereas stringers zones are 2, 6 and 7.

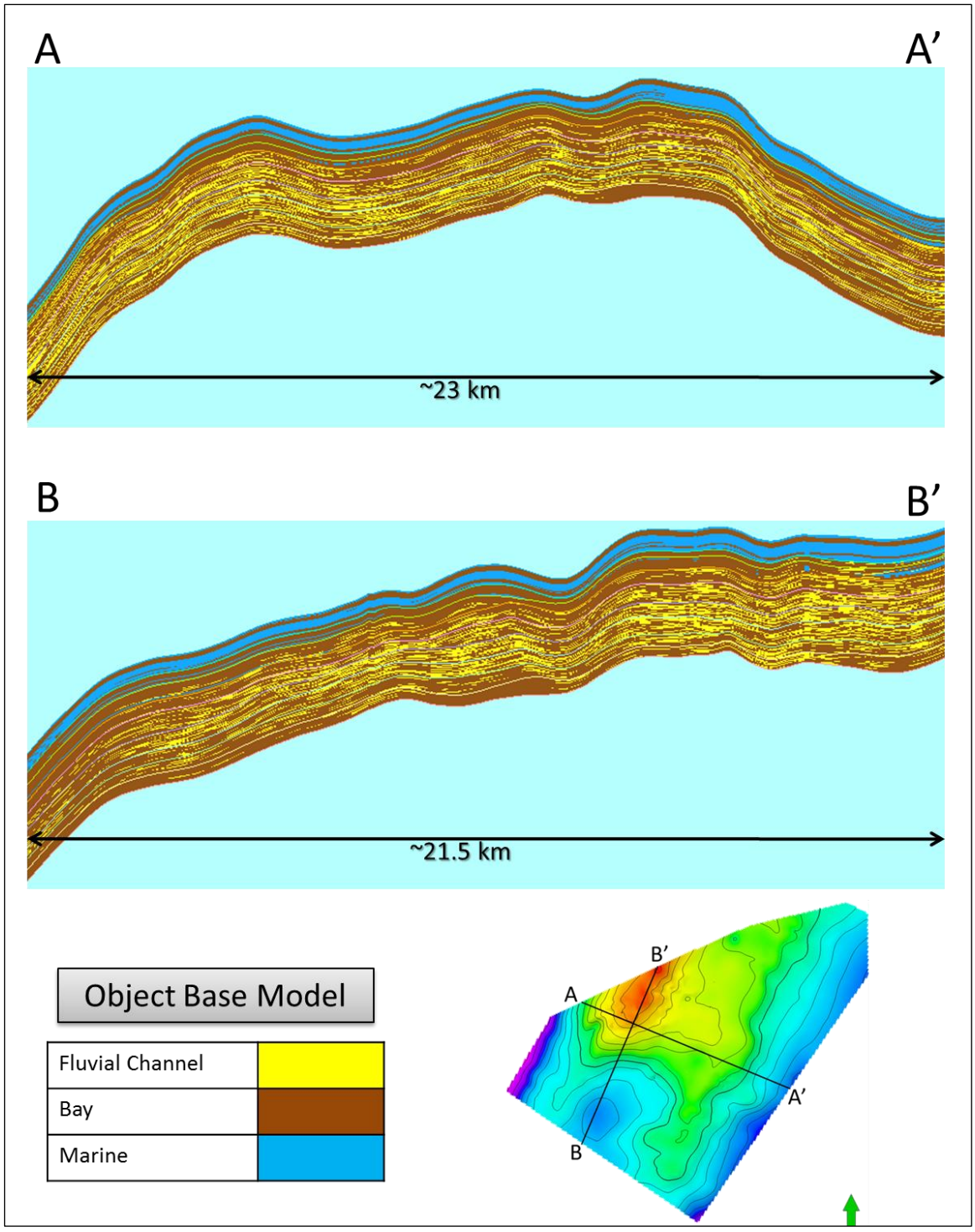

Figure 31 Two cross sections cutting across object base model where the facies distribution looks unrealistic because the main sand zones are expected to have more sand channels that are thicker and more homogeneous than how it is represented in the 3D model.

4.4 Hybrid Model

In general, the facies in the zones other than the main sands are laterally more continuous and do not have specific geometries or shapes that can be modeled using objects. Two attempts to model Mauddud and Safaniya members using a hybrid approach were done.

The first approach was to construct the same object model as in previous section (4.2) and the previously built indicator kriging model was used as the background instead of the constant bay facies. This approach increased the prediction successes from 65.3% (when only object modeling was used) to 69.8% with the hybrid approach.

The second attempt was to model the main sand zones (3, 4 and 5) using objects with indicator kriging model background. Other zones were modeled with indicator kriging algorithm. The prediction success enhanced slightly to 70.3%. The 3D model looked more geologically acceptable especially in Mauddud carbonate where it is more laterally continuous. Also, the main sand zones looked geologically better with the channels objects included (Figures 30 and 31).

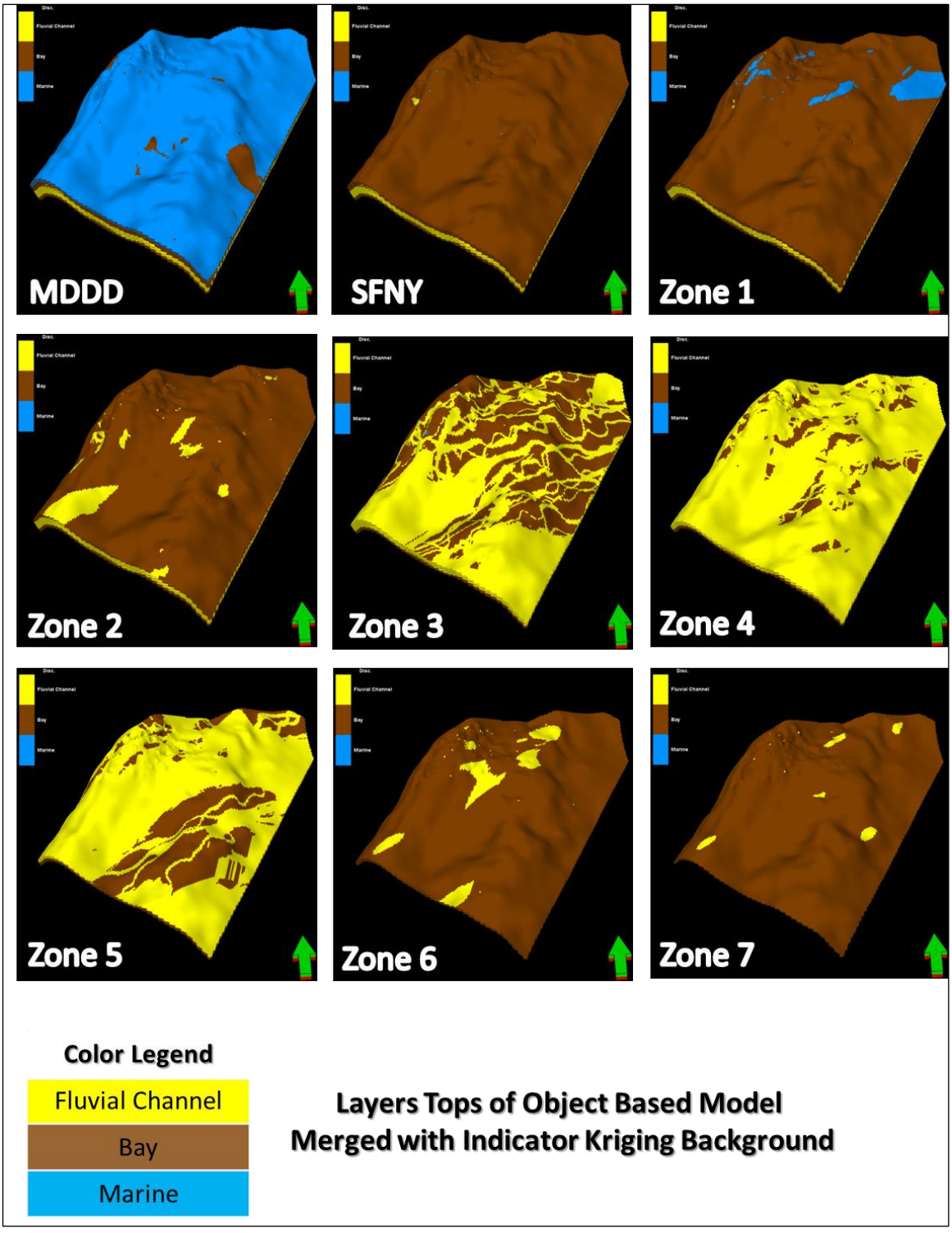

Figure 32 Top view of each modeled zone using object modeling in combination with indicator kriging algorithm. Main sand zones are 3, 4 and 5 whereas stringers zones are 2, 6 and 7.

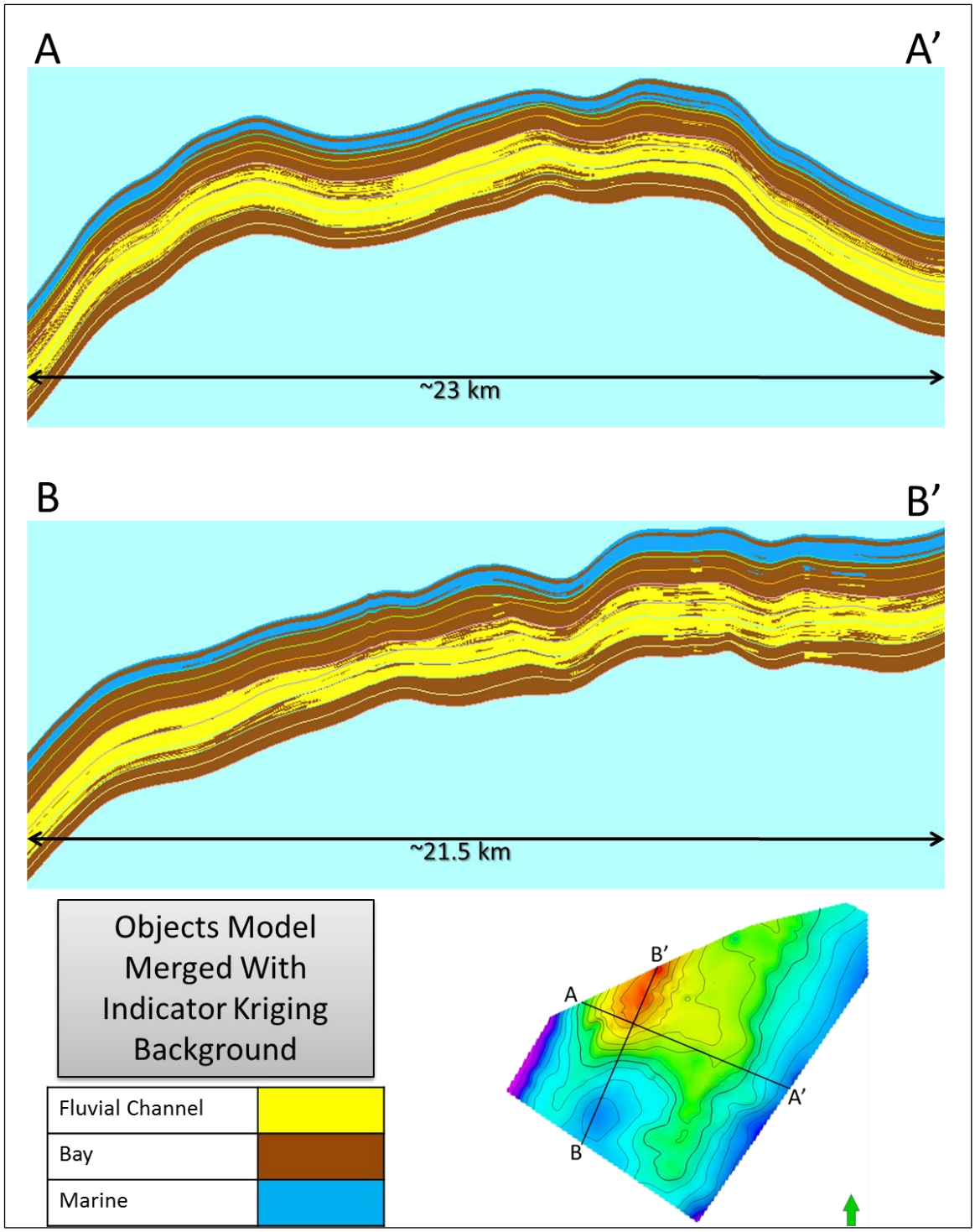

Figure 33 Two cross sections cutting across the hybrid model where the facies distribution looks more realistic since the main sand bodies include channel objects and the carbonate of Mauddud and shale in the other zones are more laterally continuous.

CHAPTER 5

CONCLUSIONS AND RECOMMENDATIONS

5.1 Summary

The Safaniya member of the Cretaceous Wasia formation contains laterally continuous and discontinuous bodies of sand intercalated with shale and silts. The main sand units of Safaniya member have continuous sandstone zones that are prolific in terms of reservoir quality. The stringers zones underlie and overlie the main sand bodies, and they may be composed by complex laterally discontinuous sand bodies.

Since the risk of drilling in the stringer zones is high; this work aims to contribute to the endeavor of mitigating risk while drilling by producing a probabilistic analysis of the occurrence of sand bodies.

This work included four major phases: a) data analysis and interpretation of classic facies using cutoffs and core data from wells b) core study of the depositional environment c) population of the depositional facies into the non-cored wells using neural

networks technique d) construction of geocellular models in Petrel software to characterize sand bodies predictability using: i) Indicator kriging, ii) Sequential indicator simulation and iii) Boolean Object-based modeling.

The six depositional facies identified from thirteen core descriptions were lumped into three general facies (fluvial channel, marine and bay) because neural network technique failed to accurately differentiate between the depositional facies that has same electrical logs characteristics. After that, the facies were populated in 188 wells that are not cored. A manual quality check and editing was performed on those populated facies to ensure consistency and accuracy.

The conceptual model of Safaniya member used in this research is basically a delta that has a source in the southwest and prograding almost toward the northeast direction. The delta mainly consists of three main parts: lower stringers, main sand and upper stringers. The clastic source was closer in the southern part of the field and generally there is less sand toward the northeast.

Safaniya member was modeled using: Indicator Kriging, Sequential Indicator Simulation, Object Modeling algorithms and one hybrid approach. Trial-and-error was the best approach to test the effect of modeling parameters in each method. Modeling parameters were tested systematically with different values and the model was then validated with thirty four well as a blind test. The predictability at best of the models came as follows: IK (74.7%), SIS (68.8%), OM (65.3%), Hybrid model (70.3%)

5.2 Conclusions

This study has arrived to the following conclusions:

- In order for the for neural network estimation technique to work properly, the categories should either have distinctive characteristic on well logs or the number of categories should not be big.
- The initial high predictability of the model which was, in general, over 65% might be due to the high density of well control. If less number of wells were present and same modeling parameters were used, the predictability might be less as well.
- Generating several realizations with same modeling parameters (i.e., lateral and vertical ranges, kriging type, objects geometries …etc) did not change the predictability significantly. The difference between highest and lowest predictability was 1.7% in the case SIS (11 realizations) algorithm and 0.6% in the case of object modeling (4 realizations).
- There were no specific parameters that affected the model predictability when IK algorithm was used. However, when OM was tested, there were two parameters that changed the predictability of the model significantly: object thickness and channel amplitude.
- Results of all models came to agree, in the very general, with the conceptual model.
- The best approach to geologically represent the reservoir facies and reduce the uncertainty could be by modeling the laterally continuous beds with IK and the discontinuous geological bodies with OM and use IK as background.

5.3 Recommendations

This research was done to test different modeling techniques and to learn from the results how to enhance the model in the future and to reduce the uncertainty associated with drilling in clastic reservoirs.

Due to time and hardware limitations; there were other methods and parameters that could be tested and experimented that were not done. This study provides some hints and recommendations to be considered for any future modeling job. The recommendations are listed based on their priority:

- The current layering scheme in Safaniya member should be revisited to reflect the most recent sequence stratigraphic and sedimentological studies. This may help in locating sand bodies that can be targeted for drilling.
- Faults must be incorporated in the model to account for any discontinuities. That may impact fluid flow in the reservoir.
- Neural network will not work well with facies that are classified based on environment of deposition and not lithology. The log response of these facies might be identical for several facies and would be not differentiable by neural network algorithm. To model all these facies; utilize the facies interpretation of cored wells and generate manual facies interpretation based in non-cored wells.
- It is highly recommended to manually check the quality and edit the output data after running any prediction or estimation technique. The time spent in this process is fully justified as it will reduce any error that is generated by the automated interpretation.

- Before modeling a geologic zone; study the geology to come up with general ideas about facies distribution and orientations. After that trial and error approach should be performed, because it may give results that are contradicting with the conceptual geological model.
- When modeling laterally continuous beds; IK or SIS techniques are recommended. OM is recommended only when modeling discontinuous facies or facies with known geometries.
- Use different semi-variogram models for each zone and for each facies as it may change the model predictability positively as opposed to using only one semi-variogram for the whole model.
- This model was built with 2 feet thick cells. It is recommended to increase the thickness to 5 feet to reduce the number of cells in the model and it will be faster to build.
- When creating objects in Petrel using adaptive channel, to connect a known channel between two or more wells. Trends could be also applied to force the channels in a direction known to be a channel built.
- Use truncated Gaussian Simulation algorithms to account for any transition between facies in one zone. This algorithm provides stochastic images of sedimentary geology in fluvio-deltaic environments.
- Create fine resolution model to account for small beds.
- In IK and SIS sittings try to use global facies fraction from well data and not from the default upscaled data.

APPENDIX A

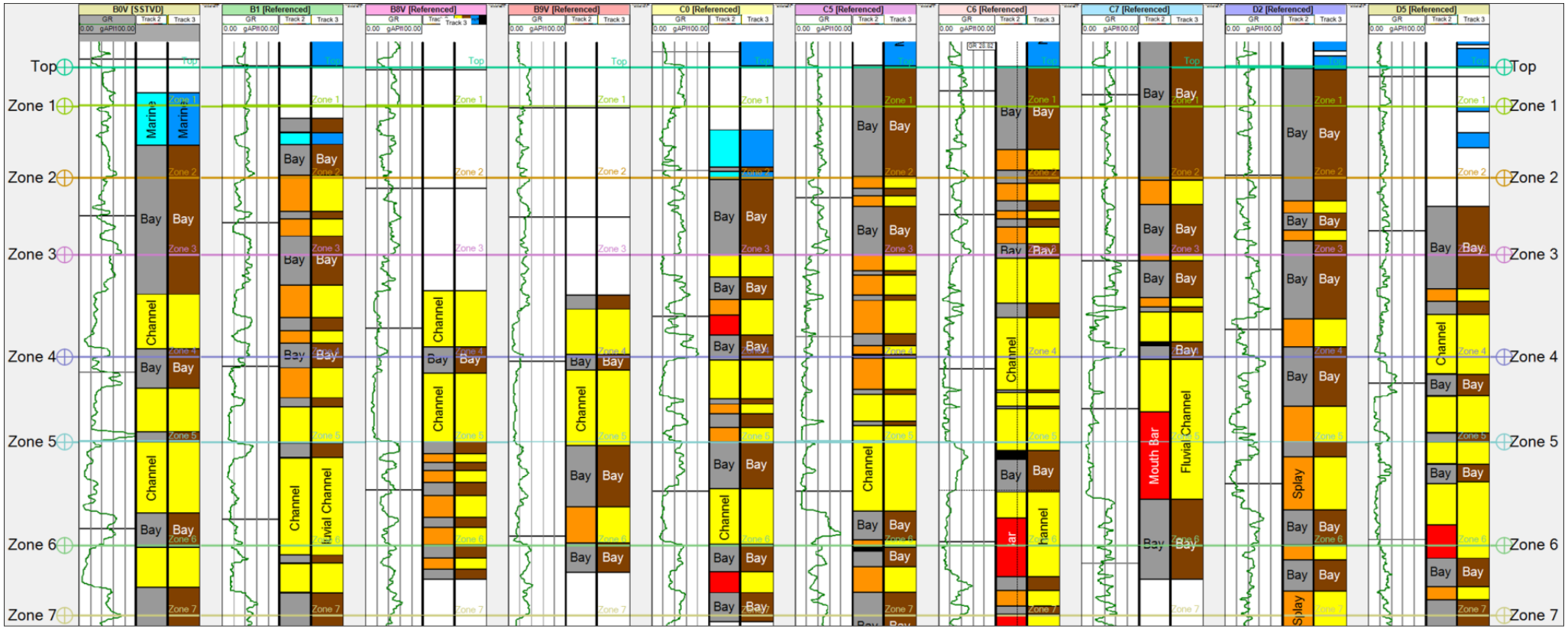

Code	Name	Color
1	Channel	
2	Splay	
3	Bay	
4	Mouth Bar	
5	Swamp	
6	Marine	

Track 2 Legend

Code	Name	Color
1	Fluvial Channel	
2	Bay	
3	Marine	

Track 3 Legend

Figure A.A1 Depositional facies from core description.
Track 1: Gamma ray log
Track 2: Originally described six facies
Track 3: Generalized three facies to ease the prediction algorithm

APPENDIX B

Artificial Neural Networks (ANN)

In simple words, Artificial Neural Networks (ANN) is a computational tool that is used to automatically find a pattern or relationships between multiple known inputs and a single unknown output (Rogers, 1992).

Technically speaking, ANN is an interconnected group of artificial software neurons that uses a mathematical or computational model for information processing based on a connectionistic approach to computation.

ANN is an adaptive system that changes its structure based on external or internal information that flows through the network.

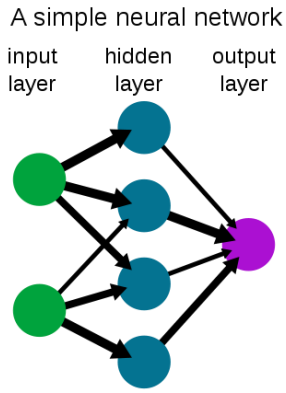

ANN is used in, but not limited to, the following areas:

- In petroleum geology: facies and logs prediction
- In computer science: speech recognition
- In business: sales forecasting and risk management
- Etc…

In facies prediction for example, the input data will be: well logs and core description. The ANN model when run; finds a relationship between well logs and interpreted facies so that it learns how to predict facies in wells that have well logs only or vice versa.

This tool is usually fast and in the petroleum industry, it is used to predict costly data that are not available in some or – sometimes – most of the wells.

APPENDIX C

Categorical Indicator Kriging

(Deutsch, 2002)

The purpose of Indicator Kriging for categorical variable is to estimate the uncertainty distribution in the categorical facies variable.

The probability distribution consists of estimations of probability for each category (facies): p*(k), k=1, …, K. The figure below shows the probability values for five facies as an example.

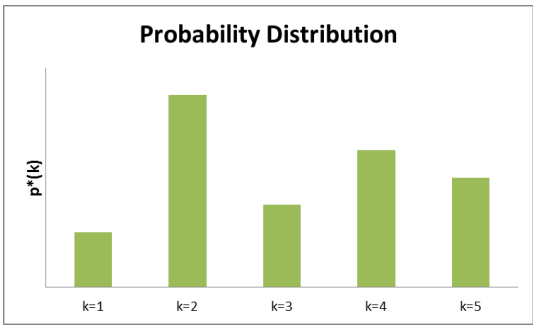

The probability values are estimated by first coding the data (facies) as indicators or probability values.

$I(u_\alpha;z_k)$ = *Prob* {facies k being present}

$$= \begin{cases} 1, if\ facies\ k\ is\ present\ at\ u\alpha \\ 0, otherwise \end{cases}$$

The anticipated value of this indicator variable is the stationary prior probability of facies k, p(k). the residual data, Y, is considered:

$$Y(u_\alpha;z_k) = i(u_\alpha; k) - p(k), \quad \alpha = 1, \ldots, n, \quad k = 1,\ldots, K$$

Kriging the residual data is used to derive the probability of each facies $k = 1,\ldots, K$ at unsampled location. The result of indicator kriging is a model of uncertainty at location **u**:

$$p_{IK}(u; k) = \sum_{\alpha=1}^{n} \lambda\alpha\ (k).[i(u_\alpha;k)-p(k)] + p(k), \quad k = 1,\ldots, K$$

APPENDIX D

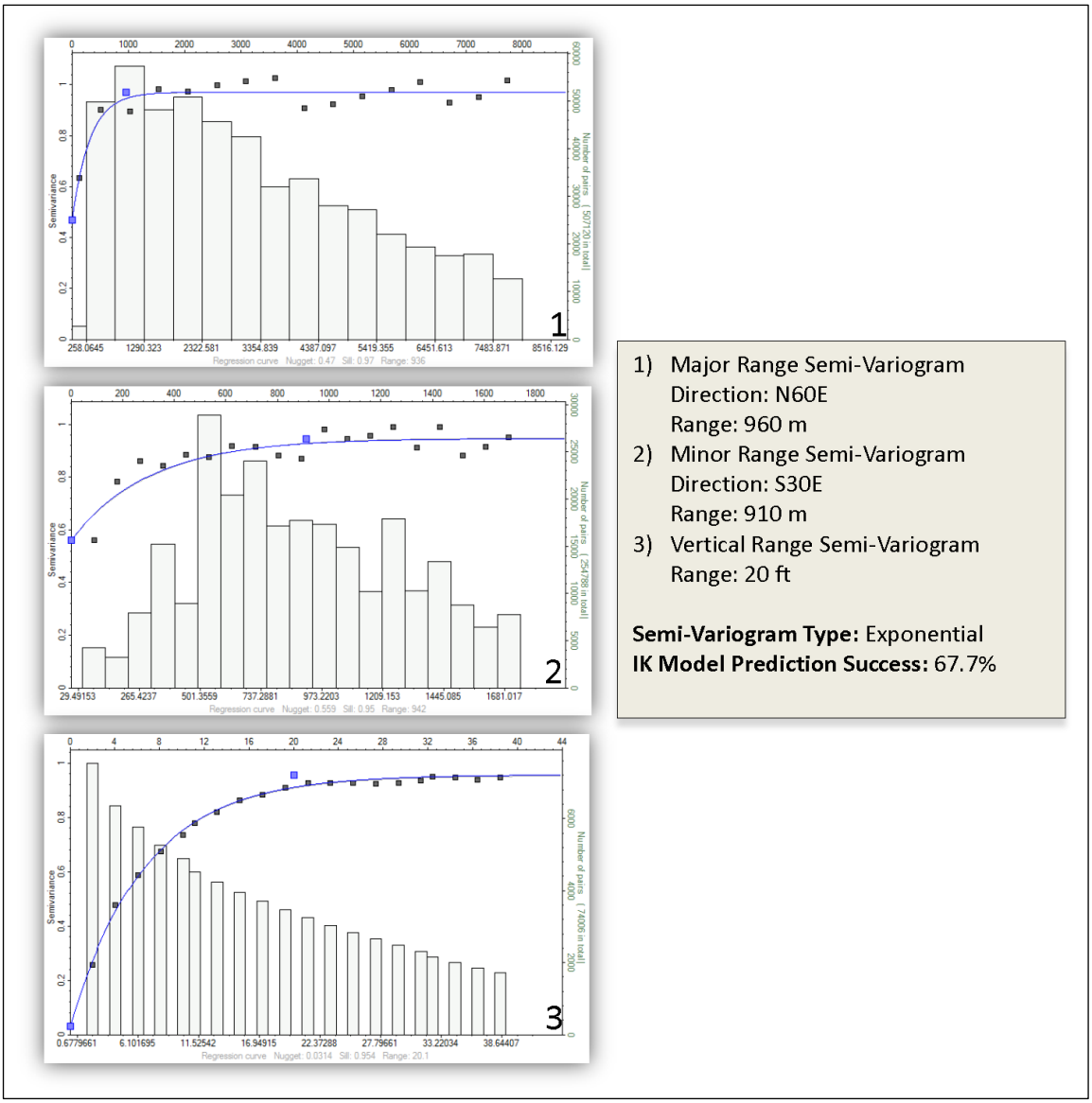

Figure A.D1 An example for semi-variogram calculated for Safaniya member (all zones combined) and the resulted IK model prediction match.

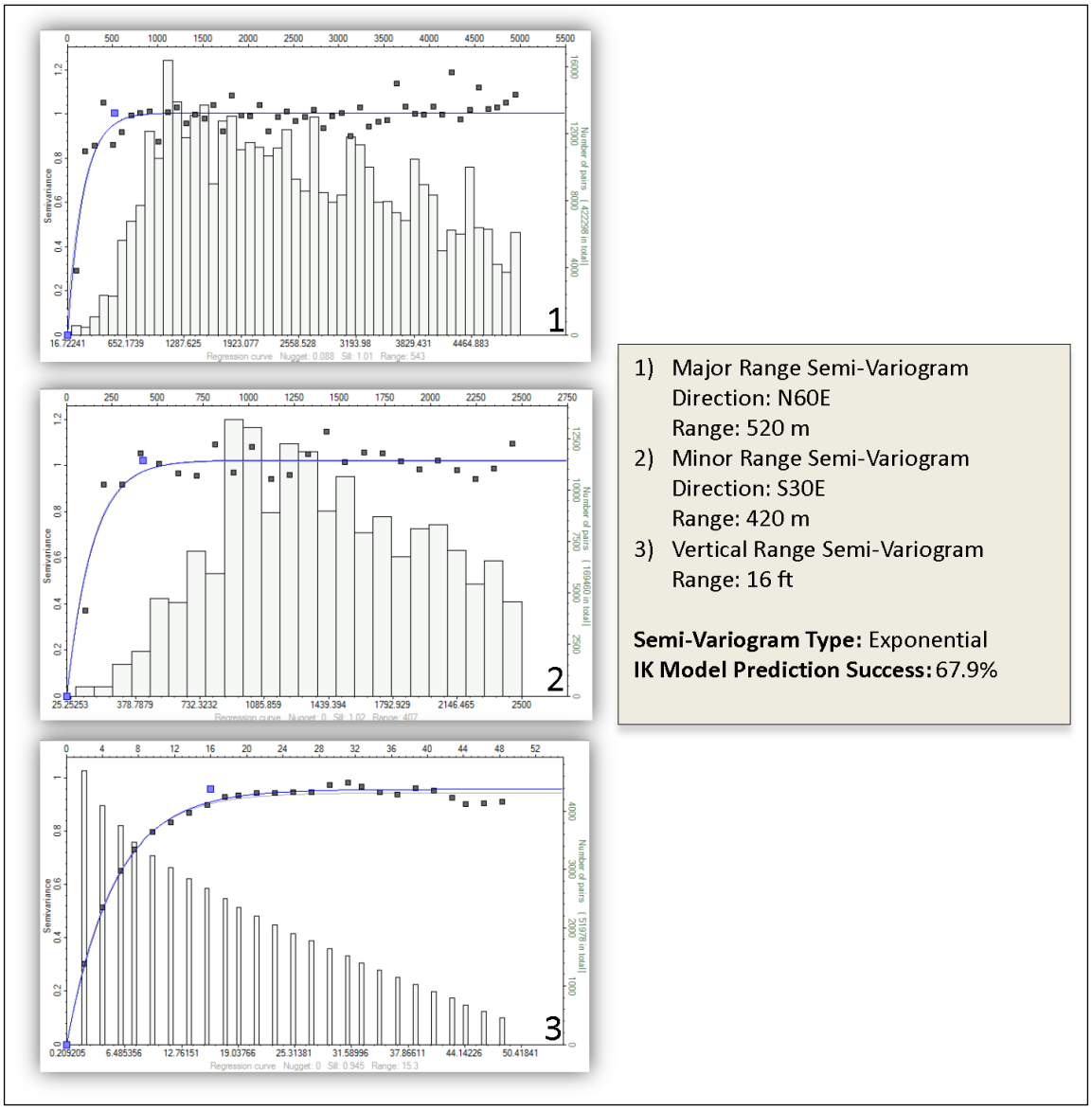

Figure A.D2 An example for semi-variogram calculated for Safaniya member (all zones combined) and the resulted IK model prediction match.

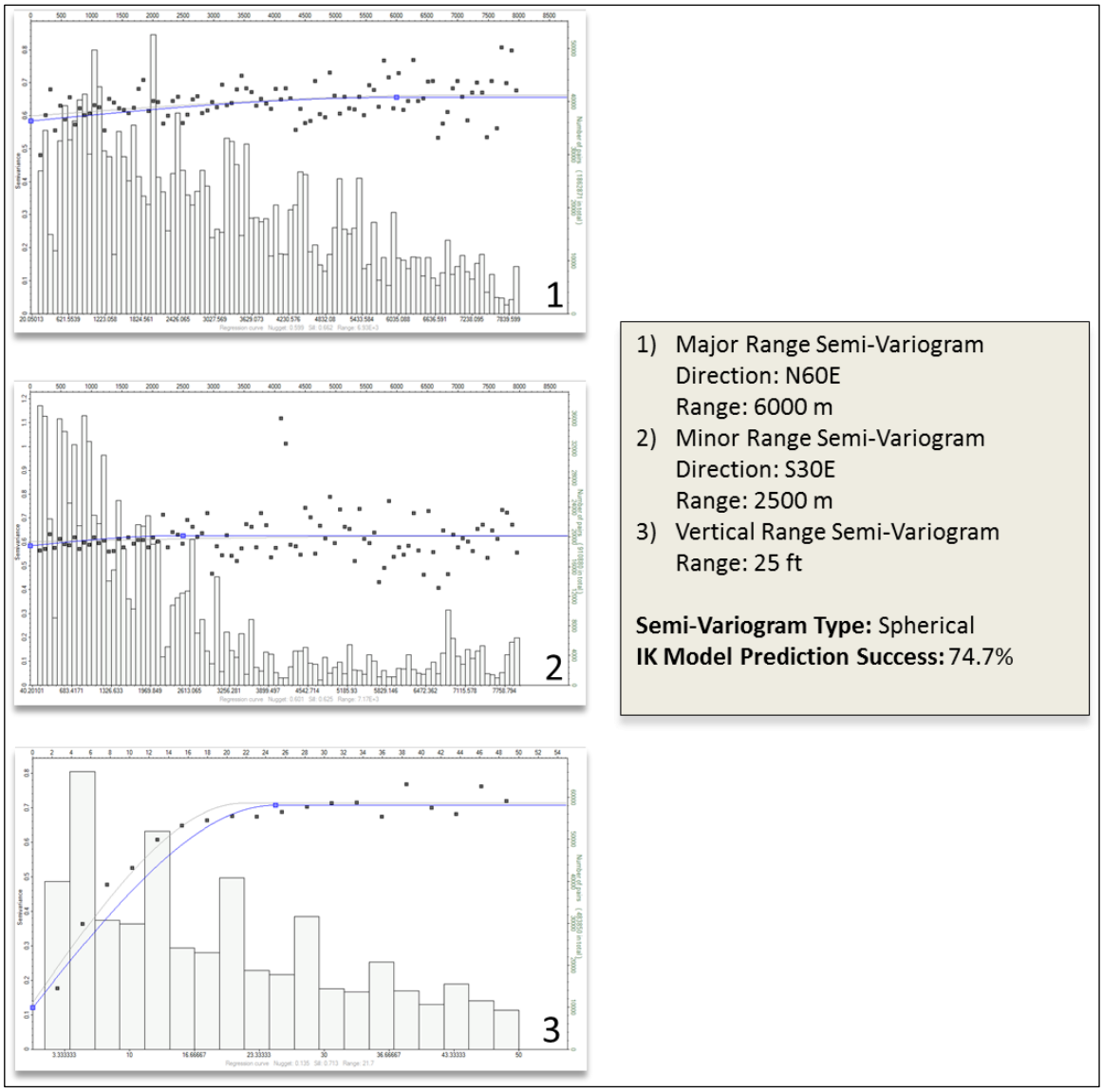

Figure A.D3 An example for semi-variogram calculated for Safaniya member (all zones combined) and the resulted IK model prediction match. The values for major, minor and vertical ranges selected here are based on trial and error approach and gave better prediction results than the previous two examples even though the semi-variogram model is having high nugget values..

APPENDIX E

Sequential Indicator Simulation

(Remy et al, 2009)

The algorithm of Sequential Indicator Simulation (SIS) goes as follows:

1. Define a path visiting all locations to be simulated

2. For each location **u** along the path:

    (a) Retrieve the neighboring categorical conditioning data: $z(u_\alpha)$, $\alpha = 1, \ldots, N$

    (b) Turn each datum h $z(u_\alpha)$ into a vector of indicator data values:

    $v(u_\alpha) = [i(z(u_\alpha), z_1), \ldots, i(z(u_\alpha), z_K)]$ The indicator variable is defined by:

$$i(\mathbf{u}, \mathrm{k}) = \begin{cases} 1 & \text{if } Z(\mathbf{u}) = \mathrm{k} \\ 0 & \text{otherwise} \end{cases}$$

    (c) Estimate the indicator random variable *I*(u; k) for each of the K categories by solving a kriging system. The simple kriging estimator is given by:

$$I^*(\mathbf{u}, \mathrm{k}) - \mathrm{E}\{\mathrm{I}(\mathbf{u}, \mathrm{k})\} = \sum_{\alpha=1}^{\mathrm{N}} \lambda_\alpha \Big(\mathrm{I}(\mathbf{u}_\alpha, \mathrm{k}) - \mathrm{E}\{\mathrm{I}(\mathbf{u}_\alpha, \mathrm{k})\} \Big)$$

    (d) The estimated values *i**(u; k) = prob*(Z(u) = k), after correction of order-relation problems, define an estimate of the discrete probability density function (pdf) $f_{Z(u)}$ of the categorical variable *Z*(u). Draw a realization from *f* and assign it as a datum at location **u**.

    (e) Loop until all locations are visited

3. Repeat the previous steps to generate another realization

APPENDIX F

Modeling Fluvial Facies Objects

(Deutsch, 2002)

Object based modeling techniques require information on size, shape, and relationship between the different objects. For braided fluvial reservoirs, some of the needed information includes:

- Fraction of channel sand (could vary areally and vertically)
- Width and thickness of channel sands (could vary vertically and follow a distribution of possible sizes)
- Measures of channel sinuosity (depend on size of channel and vertical position)
- Geometry of channel "families" or multi-story channels

The figure below illustrates one possible conceptual model for fluvial facies. There are four facies types where the geometric specification of each is chosen to mimic shapes idealized from observation.

1) The first facies type is impermeable background floodplain shale, which is viewed as the matrix within which the reservoir quality or sand objects are embedded.
2) The second facies type is channel sand that fills sinuous abandoned channels. This facies is viewed as the best reservoir quality due to the relatively high energy of deposition and consequent coarse grain size. There may be special features within the channel sands such as (1) heterogeneous channel fill, perhaps containing some fine-grained non-net material, (2) a channel lag deposit at the base, and (3) fining-upward trends within the channel fill.
3) The third facies type is levee sand formed along the channel margins. These sands are considered to be poorer quality than the channel fill.
4) The fourth and final facies type is crevasse splay sand formed during flooding when the levee is breached and sand is deposited away from the main channel. These sands are also considered to be poorer quality than the channel fill.as illustrated below; crevasses often form where the channel curvature is high.

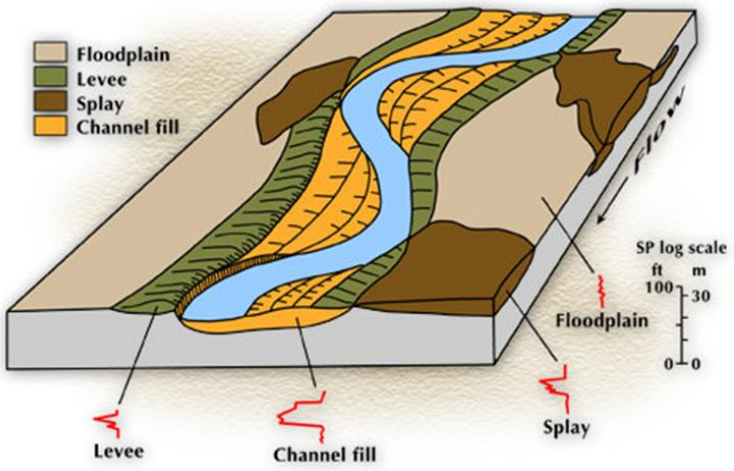

REFERENCES

Al-Ghamdi, Abdulla H., Rayed M. Al-Zayer, Isa A. Al-Samin and Abdulaziz A. Al-Gattan 2001. *Interpretational Complexities and Operational Complications Affecting Pressure Transient Analysis in Zuluf Field, Saudi Arabia.* Society of Petroleum Engineers, SPE 71576, p. 1-11.

Ali, J.K. 1994. *Neural Networks: A New Tool for the Petroleum Industry?.* Society of Petroleum Engineers, SPE 27561, p. 217-231.

Al-Khalifah, M. and M. Makkawi 2002. *The Impact of Data Integration on Geostatistical Porosity Modeling: A Case Study from the Berri Field, Saudi Arabia.* Journal of Petroleum Geology, vol. 25, no. 4, p. 485-498.

Al Maskeen, Abdul Mohsen A. 2007. *Advanced Geological Modeling and Uncertainty Analysis in a Complex Clastic Gas Reservoir from Saudi Arabia.* Society of Petroleum Engineers, SPE 109275, p. 1-17.

Al-Sabti, H.M. and K.A. Al-Bassam 1993. *3-D Electrofacies Model, Safaniya Reservoir, Safaniya Field, Saudi Arabia.* Society of Petroleum Engineers, SPE 25611, p. 155-169.

Armstrong, Margaret 1998. *Basic Linear Geostatistics.* Springer, USA, 155 p.

Brandsæter, Inge, HanneTherese Wist, Arve Næss, Oddvar Lia, Ole Arntzen, Philip S. Ringrose, Allard W. Martinius and Thomas Rage Lerdahl 2001. *Ranking of Stochastic Realizations of Complex Tidal Reservoirs Using Streamline Simulation Criteria.* Petroleum Geoscience, vol. 7, p. S53-S56.

Busch, D. A. and D. A. Link 1985. *Exploration Methods for Sandstone Reservoir.* OGCI Inc., USA, 327 p.

Chevron Exploration and Production Service Company 1990. *Geology of the Safaniya Reservoir, Safaniya field.* Volume 1. Saudi Aramco internal report.

Contreras, A., C. Torres-Verdin, K. Kvien, T. Fasnacht and W. Chesters 2005. *AVA Stochastic Inversion of Pre-Stack Seismic Data and Well Logs for 3D Reservoir Modeling.* EAGE 67th conference, T-15, p. 1-5.

Deutsch, Clayton V. 2002. *Geostatistical Reservoir Modeling.* Oxford University Press, USA, 376p.

Deutsch, Clayton V. and André G. Journel 1998. *GSLIB: Geostatistical Software Library and User's Guide.* Oxford University Press, USA, 369p.

Dubrule, O. 1998. *Geostatistics in Petroleum Geology.* AAPG, USA, course notes series #38.

Georgsen, F., A.R. Syversveen, R. Hauge, J.I. Tollefsrud and M. Fismen 2008. *Local Update of Object-Based Geomodels.* Society of Petroleum Engineers, SPE 113532, p. 1-9.

Gibling, Martin R. 2006. *Width and Thickness of Fluvial Channel Bodiesand Valley Fills in the Geological Record: A Literature Complication and Classification.* Journal of Sedimentary Research, v. 76, p. 731-770.

Gilgen, Hans 2006. *Univariate Time Series in Geosciences: Theory and Examples.* Springer, USA, 718 p.

Glacken, Ian M. and P. C. J. Blackney. *A Practitioners Implementation of Indicator Kriging.* The Geostatistical Association of Australasia "Beyond Ordinary Kriging" Seminar. 1998.

Goovaerts, P. 1997. *Geostatistics for NaturalR Evaluation.* Oxford University Press, USA, 496 p.

Haq, B.U., J. Hardenbol and P.R. Vail 1988. *Mesozoic and Cenozoic Chronostratigraphy and Cycles of Sea-Level Change.* In, C.K. Wilgus, B.S. Hastings, C.G. St. C. Kendall, H. Posamentier, J. Van Wagoner and C.A. Ross (Eds.), Sea-level changes: an integrated approach. Society of Economic Paleontologists and Mineralogists, Special Publication 42, p. 71–108.

Hashem, Mohamed, Randy Miller, Saleh M. Dossari, Parvez Butt, Raza Hassan and Sadiq Hussain 2008. *Enhanced Reservoir Contact Using New LWD Technology in Thin Channel Sands.* Society of Petroleum Engineers, SPE 113779, p. 1-13.

Hasson, Richard C, Darwin O. Hemer, John F. Mason, and Quentin M. Moore 1977. *Petroleum Development in Middle East Countries in 1976.* AAPG Bulletin, v. 61, no. 10, p. 1795-1829.

Hohn, Michael Edward 1998. *Geostatistics and Petroleum Geology*. Kluwer Academic Publishers, USA, 248 p.

Isaaks, Edward H. and R. Mohan Srivastava 1989. *An Introduction to Applied Geostatistics.* Oxford University Press, USA, 592 p.

Journel, A.G., 1983. *Nonparametric Estimation of Spatial Distributions.* Mathematical Geology 15 (3), 445–468.

Macrides, C.G. and F.A. Neves 2008. *Lithology Estimation from a Multicomponent 3D-4C OBC Seismic Survey Over a Clastic Reservoir in the Arabian Gulf.* GeoArabia, v.13, no.1, p.15-34.

Marinoni, O. 2003. *Improving Geological Models Using a Combined Ordinary – Indicator Kriging Approach.* Engineering geology 69 (2003), 37-45.

Mashadi, M.M. 1998. *Safaniya Reservoirs Summary Project.* Saudi Aramco in-house unpublished report.

Olariu, C. and Janok P. Bhattacharya 2006. *Terminal Distributary Channels and Delta Front Architecture of River-Dominated Delta Systems.* Journal of sedimentary research, v. 76, p. 212-233.

Pettijohn, F.J., Paul Edwin Potter and Raymond Siever 1987. *Sand and Sandstone.* Springer, USA, 553 p.

Qi, Lianshuang, Timothy R. Carr and Robert H. Goldstein 2007. *Geostatistical Three-Dimensional Modeling of Oolite Shoals, St. Louis Limestone, Southwest Kansas.* AAPG Bulletin, v. 91, no. 1, p. 69-96.

Remy, Nicolas, Alexander Boucher and Jianbing Wu. 2009. *Applied Geostatistics with SGeMS: A User's Guide.* Cambridge University Press, UK, 264 p.

Rider, M. 1996. *The Geological Interpretation of Well Logs.* Gulf Publishing Company, UK, 280 p.

Rogers, Sammuel J., J.H. Fang, C.L. Karr and D.A. Stanley 1992. *Determination of Lithology from Well Logs Using a Neural Network.* AAPG Bulletin, v.76, no. 5, p. 731-739.

Saggaf, M.M. and E.L. Nebrija 2000. *Estimation of Lithologies and Depositional Facies from Wire-Line Logs.* AAPG Bulletin, v. 84, no. 10, p. 1633-1646.

Saggaf, M.M. and E.L. Nebrija 2003. *A Fuzzy Logic Approach for the Estimation of Facies from Wire-Line Logs.* AAPG Bulletin, v. 87, no. 7, p. 1223-1240.

Schlumberger Information Solutions 2009. *Property Modeling.* Course notes, 503 p.

Sharland, P.R., R. Archer, D.M. Casey, R.B. Davies, S.H. Hall, A.P. Heward, A.D. Horbury and M.D. Simmons 2001. *Arabian Plate Sequence Stratigraphy.* GeoArabia Special Publication 2, Gulf PetroLink, Bahrain, 371 p., with 3 charts.

Soliman, Osama M. 2009. *Sedimentology of the Khafji and Safaniya members, Offshore Fields, Saudi Arabia.* Saudi Aramco internal report.

Strebelle, S. 2002. *Conditional Simulation of Complex Geological Structures Using Multiple-Point Statistics.* Mathimatical geology, v. 34, no. 1, p. 1-21.

Tye, S.T. 2004. *Geomorphology: an Approach to Determining Subsurface Reservoir dimensions.* AAPG Bulletin, v. 88, no. 8, p. 1123-1147.

Vargas-Guzman, J.A. and Hisham Qassab 2006. *Spatial Conditional Simulation of Facies Objects: Modeling a Complex Clastic Gas Reservoir.* Journal of petroleum science and engineering 54, p. 1-9.

Ziegler, M.A. 2001. *Late Permian to Holocene Paleofacies Evolution of the Arabian Plate and its Hydrocarbon Occurrences.* GeoArabia, v. 6, no. 3, p. 445-505.

VITA

Ahmad Atig Mubarak Al-Dossary was born in Al-Ahsa, Kingdom of Saudi Arabia, in May 29th, 1978. He joined King Fahd University of Petroleum and Minerals in September 1996 and earned his B.Sc. degree in geology in August 2002. In April 2003 he joined Saudi Aramco in Dhahran and started his career as an operation geologist handling field development operations in northern offshore fields for five years. He was also part of several multi-disciplinary teams that conducted key projects in different oil fields such as Safaniya, Berri and Abu Sa'fah.

Ahmad joined the Master degree program as a part-time and received his M.Sc. in Geology in May 2013.

Address: Saudi Aramco, P.O. Box 2527, Dhahran 31311, Saudi Arabia.

Email: ahmad.dossary@gmail.com